ATTRIBUTE BASED COMPARISON OF COOLING TECHNIQUES AND CFD SIMULATION OF SPRAY

A
Thesis

submitted in partial fulfillment of the requirements for the award of degree of

Master of Engineering (M.E.)

In
Thermal Engineering

Submitted by
ANAM SINGH
(ROLL NO. 801383004)

UNDER THE GUIDANCE OF

DR. V. P. AGRAWAL
(Visiting Professor)

DEPARTMENT OF MECHANICAL ENGINEERING
THAPAR UNIVERSITY, PATIALA – 147004

JULY 2015

CERTIFICATION

I, Anam Singh declare that this thesis report entitled "***Attribute Based Comparison Of Cooling Techniques And CFD Simulation Of Spray***", submitted towards fulfillment of the requirements for the award of Master's Degree in Thermal Engineering, in Mechanical Engineering Department of Thapar University, Patiala, is entirely my own work. This document has not been submitted for any degree in any other institution.

Date: 15/07/2015

Place: PATIALA

Anam Singh

801383004

Thapar University, Patiala

This is to certify that above statement made by the candidate is correct and true to the best of my knowledge.

DR. V. P. AGRAWAL

(Visiting Professor)

Mechanical Engineering Department

Thapar University, Patiala

Countersigned by

Dr. S.K. Mohapatra

Sr. Professor and Head

Mechanical Engineering Department

Thapar University, Patiala

Dr. S.S. Bhatia

Dean

Academic Affairs

Thapar University, Patiala

ACKNOWLEDGEMENT

I would like to express my deepest gratitude to my supervisor, Dr. V. P. Agrawal, for his excellent guidance, caring, patience, and providing me with an excellent atmosphere for doing research. Your advice on both research as well as on my career have been priceless. The opportunity, support, exposure and atmosphere provided by the Thapar University, Patiala, to carry out my studies are highly appreciated.

A special debt of gratitude is owed to the authors whose works I have consulted and quoted in this work. Last but not least, I am forever grateful to my parents, family and friends for their unconditional support and best wishes.

Content

List of figures

List of tables

Nomenclature

h: - convictive heat transfer coefficient

A_s: - Surface area

θ_{lmtd}: - Log mean temperature difference

Nu: - Nusslet number

k: - conduction heat transfer coefficient

D_h: - Hydraulic diameter

g: - height of microchannel

w: - width of microchannel

f: - friction factor

Re: - Reynolds number

v: - velocity

Q: - Volumetric flow rate

q''_m : - Critical heat flux

ρ: - Density

h_{fg} : - latent heat of vaporization

$\bar{Q}''$: - Mean volumetric flux across impact area of spray.

d_{32} : - Sauter mean diameter

σ: - Surface tension

C_P : - Specific heat at constant pressure

ΔT_{sub} : - Fluid subcooling at nozzle inlet

L : - Length

α : - Inclination angle between spray axis and normal to test surface

θ: - Spray cone angle

dA': - Differential area measured along spherical surface.

dA : - Differential area measured along test surface

ms:- Mili second

Subscripts

f: - fluid

g: - liquid

s: -spray cooling

m: - microchannel cooling

Abstract

High heat transfer techniques are requirement of today's electronic industry and in this research four high heat transfer techniques spray cooling, jet impinging cooling, two phase microchannel flow cooling technique and single phase microchannel flow cooling techniques are compared on the basis of attributes. In this way the collective approach using multiple attributes are taken to compare the four techniques. To compare the cooling techniques first the different attributes on which the selection of cooling technique depends are collected, then they classified into two broad categories: General Attributes and Specific attributes. Each category is further divided into groups and then subgroups. The codification scheme is also given to codify the attributes. The techniques are compared using MADM-CCSD approach by which16 different experimental results (4 experiments related to each cooling technique) are used to compare the cooling techniques and Jet impinging technique is best among all four techniques.

In next section the CFD simulation of spray has been done using DPM (Discrete phase modeling) in ANSYS Fluent commercial software. In this way the simulation is first optimized to use less computer resources without affecting the results. Variation of spray angle, number of nozzles and distance between multiple number of nozzles have been studied on wall film mass, wall film height, uniformity index of wall film and velocity of wall film.

CHAPTER 1. Introduction

From the very beginning of evolution of computer chips there is always a need of cooling of the chips. As the density of transistors on chips increases the demand of new high heat flux cooling techniques comes into picture. Chip sizes are decreasing and which further needs compact high heat flux techniques to cool them. This was reported by Shankar Krishnan et al. (2007). Shankar Krishnan et al. (2007) showed that the heat dissipating density for future chips will be 200 Watt/cm^2. The same was also explained by Yang et al. (1996) in context of data centers that there is a flux requirement of high heat flux cooling techniques which are able to transfer 100W/cm^2. Lowering the chip temperature by increasing the heat transfer rate using spray cooling in electronic chips leads to decrease in leakage current and also increases the life of chip Cader et al. (2004). Moreover lowering the chip temperature leads to low resistance, increase in reliability and decrease in current leakage R. R. Schmidt and B. D. Notohardjono (2002). This shows that there is a requirement of high density heat dissipating system.

As explained in Cengel e Boles (2003) there are different conventional heat transfer techniques which are used according to their heat transfer rate and temperature range.

Cooling Technique	**Temperature range ($°C$)**	**Heat transfer range (W/cm^2)**
Natural conviction and radiation	10-1000	.01-.4
Forced conviction	2-1000	.01-2
Direct immersed natural conviction (Fluorocarbons)	1-20	.03-1
Water forced conviction	1-40	.3-20
Immersed boiling (Fluorocarbons)	4-10	.4-8

Table 1 Comparison of different cooling techniques Cengel e Boles (2003)

It has been observed from the Table 1 that the conventional heat transfer techniques are not enough to handle the heat transfer load in the case of modern computer chips. Besides the conventional cooling techniques there are various cooling techniques for cooling of computer chips are Microchannel heat sinks (single phase fluid flow), Microchannel heat sinks (two phase fluid flow), Jet impinging method and Spray cooling method. High heat transfer rate (500-1000W/cm^2) is also reported using spray cooling by Lin and Ponnappan (2003) and Pais et al. (1992). Apart from that benchmark of heat transfer 1000 W/cm^2 is achieved in laboratory using microchannels by Dan Faukner et al.
This shows the possibility of application of these modern cooling techniques in case of future computer chips. But there are many constraints on these techniques like size, compactness, performance and reliability appears as these techniques applied practically.

1.1 Single phase microchannel flow cooling

Microchannels are the channels having hydraulic diameter 200microns-10microns. In the single phase flow heat transfer the coolant increase its sensible heat in microchannel and then cooled in condenser and flow back with the help of pump. This is active cooling technique uses pump work to flow the coolant through microchannel. Temperature non uniformity is one of the major flaws of single phase microchannel cooling.

1.2 Two phase microchannel flow cooling

The main difference in single phase and two phase microchannel flow cooling is the latent heat which is absorbed by the coolant to vaporize and again condense back in condenser. In this way the pressure drop decreases but the volume handled by compressor increases due to decrease in density of vapor. A benchmark of heat transfer 1000 W/cm^2 is achieved in laboratory using microchannels by Dan Faukner et al.

1.3 Jet impinging cooling

This is the technique in which the fluid is forced through nozzle to increase the velocity and strike to hot surface to cool it. In this way the single jet or array of jet is used to increase the heat transfer coefficient. Either single phase or two phase heat transfer may be possible.

1.4 Spray cooling

Spray cooling is one of the prominent heat transfer technique which leads to very high heat transfer rate and due to that it is used in high heat producing electronic chips as well as devices like CRAY-X computers, lasers, radars and in laser medical surgeries. In this technique the high pressure liquid changed into fine droplets by passing through nozzle and these droplets strike on the hot surface and formation of thin layer takes place. Heat transfer takes place through this layer by conduction conviction and boiling. This technique is still in experimental stage and different researches are going on to optimize it as well as understanding the physics behind it. Besides that in lasers, radars and high power electronic systems the high heat flux rates are required to remove the heat. This shows the potential of these high heat flux techniques. High heat transfer rate (500-1000W/cm^2) is also reported using spray cooling by Lin and Ponnappan (2003) and Pais et al. (1992).

All these cooling techniques are yet in experimental phase and before application of these techniques in practical there is a requirement of comparison of these techniques. Sidy Ndao et al. showed in the studies that multi objective approach is rather helpful then single objective approach for comparison of these cooling techniques. Because there are many variables on which these techniques depends. Further each cooling technique depends on specific variables and these variables are required to be optimized to get the efficient results considering variables related to electronic chips.

Apart from comparison the detailed dependence of spray cooling is yet to be studied. In this way the effect of spray angle and multiple numbers of nozzles at varied distance between nozzles on mass of wall film have been studied in this research.

1.5 Objectives

In the nutshell the two different aspects have been covered in this study

- The different cooling techniques have to be classified on the basis of attributes and codify them so that it is easier to implement the cooling technique practically.
- Multi-objective comparison between various high heat transfer techniques has to been done.
- The dependence of change in nozzle angle, multiple nozzles and nozzles at varied distances on wall film mass in the case of spray cooling have to be studied.

CHAPTER 2. Literature review

In this chapter there are two sections in first section the literature review related to comparison of spray cooling is done and in next section the literature related to CFD simulation of spray cooling is discussed.

2.1 Literature review related to comparison of spray cooling

In this way the basic definition as well as the previous literature review is discussed in details in this section of the chapter. The various cooling techniques for cooling of computer chips are direct pool boiling (Thermosyphon), Miniature loop heat pipe, Microchannel heat sinks(single phase fluid flow), Microchannel heat sinks(two phase fluid flow), Vapor compression cycle using simple heat sink, Vapor compression cycle using microchannel heat sink, Jet impinging method and Spray cooling method. There are different attributes which govern all these techniques and on basis of these attributes we compare them according to the importance of each attribute in different applications so that it is easy for anybody to select and apply these techniques according to need.

The above approach made by P.P. Bhangale et al. (2004) and they collected different attributes governing a robot and code them and select pertinent attributes to compare different robots on basis of their importance by MADM approach. Similar approach was taken by D.P. Singh et al. (2013) and they compare different types of heat exchangers for specific operation. The same approach was used by Mehrdad Alemi et al. (2010) to select the artificial lift in different types of oil fields on the basis of TOPSIS model and also developed a software model on basis of this model.

One of the critical steps in MADM technique is calculation of weight given for each attributes. There are many methods given by different authors to calculate the weights of attributes like manual method P.P. Bhangale et al. (2004) and D.P.Singh (2013) concurrent approach G. Naga Balaji Kiran et al. (2013) etc. These methods are highly dependent on human thinking and previous experience. But the new approach called CCSD approach Ying-Ming Wanga (2010) is used to calculate the weights which is also called correlation coefficient, standard deviation. The previous methods are not linked with values but the CCSD approach Ying-Ming Wanga (2010) is directly linked with the values of attributes, standard deviation

(SD) of attributes and correlation coefficient (CC) which is factor of effect of removing each attribute from overall assessment. In this way the correlation coefficient is depend on standard deviation of values of each attribute.

2.1.1 Shankar Krishnan et al. (2007)

Shankar Krishnan et al. showed that the heat dissipating density for future chips will be 200 Watt/cm2. This shows that there is a requirement of high density heat dissipating system.

2.1.2 Cader et al. (2004)

Cader et al. showed that lowering the chip temperature by increasing the heat transfer rate using spray cooling in electronic chips leads to decrease in leakage current and also increases the life of chip.

2.1.3 Lin and Ponnappan (2003)

Lin and Ponnappan achieved high heat transfer rate 500W/cm^2 is also reported using multi-nozzle spray cooling with water as a cooling fluid on 2 cm^2 plate as a heater. In this way this experimental value set a benchmark of high heat transfer using multiple nozzles.

2.1.4 Pais et al. (1992)

Pais et al. obtained the heat transfer rate of 1200W/cm^2 using air pressure atomized spray nozzle and the film thickness is of range 1micron and using water as a coolant. In this way the heat transfer rate was obtained at lower subcooling.

2.1.5 Pautsch et al. (2004)

Pautsch et al. has studied measured the film thickness using pressure swirl full atomizer spray with single nozzle and array of nozzles. In that study the author shows that film thickness is between 152 and 150 microns by experimental and numerical method.

2.1.6 Sivakumar and Tropea (2002)

Sivakumar and Tropea also studied the spray cooling and justified the film thickness between 55 to 192 microns.

2.1.7 Issam Mudawar (2001)

Issam Mudawar compared different cooling schemes like pool boiling, microchannel heat sinks, channel flow boiling, jet impinging cooling and spray cooling. Different cooling fluids and there thermo-physical properties like saturation temperature, liquid density, vapor density, latent heat of vaporization and surface tension was also compared in this this research. These properties of fluids are very important in thermal and flow characters and they perform different in different environments. It also explained effect of contact angle (depends on surface tension) on nucleate boiling in Thermosyphons. It also explained that for high heat transfer coefficient the smaller hydraulic diameter is required but the smaller hydraulic diameter leads to higher pressure drop and in the case of two phase heat transfer as the channel length increases leads to increase in pressure drop.

It is also explained the effect of micro texturing, mini texturing and surface orientation on CHF in the case of pool boiling (Thermosyphons). In his work it is also explained the effect of flow velocity, subcooling and microchannel surface orientation. It also explained the effects of upstream increase in temperature, bubbles and dryness fraction on downstream CHF. It shows higher sensitivity to orientation at smaller velocities and low subcooling in case of two phase flow in microchannel. This is because of bouncy force comes into picture. Surface orientation leads to vapor counter flow, vapor stagnation and no contact of liquid with heated surface which results in lowering the values of CHF. Moreover it describes that curvature of microchannel shows significant effect on CHF as the centripetal forces increase contact of fluid with surface.

Increased flow length of channel leads to decrease in CHF. Smaller cross-sectional area of microchannel shows enhancement in CHF.

It also explained the effect of jet velocity, subcooling, jet width and jet height on CHF in jet impinging cooling system.

It is also explained about dependence of CHF in spray cooling on nozzle to surface distance, flow rate and subcooling.

It also explained some phenomenon like incipience temperature drop which is undesirable in the case of chip cooling and is dominant in the case of Thermosyphons and spray cooling. Flow instabilities like vapor stagnation and counter flow which leads to transient flow is dominant in multiple microchannels. Temperature uniformity over the chip surface which cannot attained by single phase microchannel flow and jet impingement cooling technique as compare to two phase microchannel flow and spray cooling. Furthermore the physical force in the case of jet impinging technique leads to non-applicability of this technique to delicate devices. Clogging problems in case of spray cooling and non-uniformity of spray patterns from same batch of nozzles lead to unreliability of spray cooling technology.

2.1.8 Satish G. Kandlikar et al. (2004)

Satish G. Kandlikar explained the dependence of heat transfer rate on heat transfer coefficient, area and temperature difference in the case of single phase flow inside microchannel.

$$Heat\ transfer\ rate = h\ A_s\ \theta_{lmtd} \qquad \text{Eq. 1}$$

Where heat transfer coefficient

h = Nu k/D_h Eq. 2

Hydraulic diameter

$D_h = \frac{4\,gw}{2(g+w)}$ Eq. 3

Nusslet number

$$\text{Nu} = 8.235(1 - 2.0421\alpha + 3.0853\alpha^2 - 2.4765\alpha^3 + 1.0578\alpha^4 - 0.1861\alpha^5)$$ Eq. 4

Where $\alpha = \frac{g}{w}$

So from these expressions this is shown that surface area A_s (which is done in the case of microchannel) should be higher and hydraulic diameter D_h should be lower for high heat transfer in the case of single phase laminar flow. Further it was shown the use of surface enhancements to increase heat transfer rate like increase surface area with pin fin, Interrupted and staggered strip fin design, Breaking boundary layer by periodic constrictions and Grooves and ridges at specific angles to flow directions. It also gives the expression of pressure drop in the case of single phase flow heat transfer in microchannel.

$\Delta p = \frac{2\,f\,L_m \rho v^2}{D_h}$ Eq. 5

Where f is given by

$$f \cdot \text{Re} = 24(1 - 1.3553\alpha + 1.9467\alpha^2 - 1.701\alpha^3 + 0.9564\alpha^4 - 0.2537\alpha^4)$$ Eq. 6

Re is the Reynolds number, D_h is hydraulic diameter and α is explained earlier

These relations show the dependence of pressure drop on length, velocity hydraulic diameter and Reynolds number, microchannel dimensions and physical properties of cooling fluid.

2.1.9 Satish G. Kandlikar et al. (2003)

Satish G. Kandlikar et al. shows the dependence of single phase laminar heat transfer in microchannels on conventional formulas.

2.1.10 Satish G. Kandlikar (2002)

Satish G. Kandlikar explained the effect of surface tension in multichannel flow boiling. It also explained the flow instabilities like vapor stagnation and counter flow which leads to transient flow is dominant in multiple microchannels.

2.1.11 Jungho Kim (2006)

Jungho Kim described about the effect of Weber number, density ratio and Jacob number on CHF in case of spray cooling. These variables further depend on flow rate, drop size, fluid properties and subcooling. It also explained that drop velocity has higher effect of CHF then drop flux and drop diameter did not have any significant effect on CHF. It also explained the effect of surface roughness, microstructures, fins and multiple nozzles on CHF in case of spray cooling. It also shows the pressure drop in spray cooling depends on nozzle type as well as flow rate.

2.1.12 Milan Visaria et al. (2009)

Milan Visaria et al. derived the relation of CHF (q''_m) with various factors including spray inclination.

$$\frac{q''_m}{\rho_g h_{fg} \bar{Q}''} = 2.3 \left(\frac{\rho_f}{\rho_g}\right)^{0.3} \left(\frac{\rho_f Q''^2 d_{32}}{\sigma}\right)^{-0.35} \left(1 + .0050 \frac{\rho_F C_{P,f} \Delta T_{sub}}{\rho_g h_{fg}}\right) \left(\frac{f_1^{0.30}}{f_2}\right) \quad \text{Eq. 7}$$

$$\bar{Q}'' = \frac{Q}{\frac{\pi}{4} L_s^2 \cos\alpha \sqrt{1 - tan^2\alpha \; tan^2\left(\frac{\theta}{2}\right)}} \quad \text{Eq. 8}$$

$$f_1 = \frac{1}{8}\left(\frac{L_s}{H}\right)^2 \frac{\cos\alpha \sqrt{1 - tan^2\alpha\ tan^2\left(\frac{\theta}{2}\right)}}{1 - cos(\theta/2)} \frac{dA'}{dA}$$ Eq. 9

$$f_2 = \frac{1}{\frac{\pi}{4}\cos\alpha \sqrt{1 - tan^2\alpha\ tan^2\left(\frac{\theta}{2}\right)}}$$ Eq. 10

$$d_{32} = 3.67\left(We_{do}^{\frac{1}{2}} Re_{do}\right)^{-0.259}$$ Eq. 11

Where Weber number (We_{do}) and Reynolds number (Re_{do}) defined with respect to pressure drop at nozzle exit.

It also shows the dependence of pressure drop on flow coefficient (depends on nozzle type) and proportional to Q^2.

2.1.13 Satish C. Mohapatra and Daniel Loikits (2005)

Satish C. Mohapatra and Daniel Loikits compare the different types of coolants used in electric cooling. Apart from thermo-physical properties they compared other factors like electric conductivity, Corrosivity etc. They divide the coolants on the basis of electric conductivity into three different parts (1) dielectric coolants (2) electrically conductive coolants (3) electrically resistive coolants. This makes the type of fluid as one attribute to cooling technology.

2.1.14 John R. Thome (2004)

John R. Thome explained in his studies that heat transfer coefficient (h) is dependent on saturation pressure, heat transfer flux, mass velocity and vapor quality in the case of two phase flow heat transfer.

2.1.15 P.P. Bhangle et al. (2004)

P.P. Bhangle collected different attributes governing a robot and codifies them and select pertinent attributes to compare different robots on basis of their importance by MADM approach.

2.1.16 D.P. Singh et al. (2013)

D.P. Singh et al. compare different types of heat exchangers for specific operation by using MADM approach

2.1.17 Mehrdad Alemi et al. (2010)

Mehrdad Alemi et al. select the artificial lift in different types of oil fields on the basis of TOPSIS model and also developed a software model on basis of this model.

2.1.18 R. Panneer Selvam et al. (2006)

R. Panneer Selvam et al. have developed the 2D numerical model of spray cooling considering the effect of surface tension, gravity and phase change between liquid and vapor phase, keeping density, viscosity and thermal conductivity as constant for each phase. In this way modeling is done for three cases (1) when bubble grow by nucleation (2) when bubble merges with upper layer of air (3) when liquid drop impact the thin boundary of bubble.

They also used the computational model to study the spray cooling phenomenon.

2.1.19 Charles R. Ortloff and Marlin Vogel (2011)

Charles R. Ortloff and Marlin Vogel have done the CFD analysis of spray cooling. A high speed camera was used to provide the test data to construct the CFD model in Flow-3D software package to study heat transfer coefficient.

Further this model is used to find heat transfer coefficient for different combinations of droplet size, droplet velocity, droplet spatial distribution in nozzle sprays, heat flux magnitude, evaporation temperature and coolant flow rate.

Further the optimization of these results is done to give high heat transfer coefficient, avoid dry out and flooding.

2.1.20 Ying-Ming Wanga, Ying Luob (2010)

Ying-Ming Wanga and Ying Luob give the new method of finding the weights of the attributes using standard deviation of the values of each attribute. In this way the correlation coefficient (CC) is found out by removing each attribute from overall assessment and finding its effect on overall assessment.

2.1.21 Paul Joseph Kreitzer (2010)

Paul Joseph Kreitzer simulates spray cooling using MATLAB programing. In this way author generates random diameter of droplets and radial flux using Monte Carlo method. Author also use time scales to simulate crater formation, vaporization and dry out.

Author correctly predicts the distribution of droplet diameter, cater formation and dry out but there is an error in values of heat transfer and temperature distribution.

2.1.22 R. R. Schmidt, B. D. Notohardjono (2002)

R. R. Schmidt, B. D. Notohardjono reviewed that lowering the chip temperature leads to low resistance, increase in reliability and decrease in current leakage.

2.1.23 Dan Faukner et al.

Dan Faukner et al. achieved 1000W/cm^2 by using microchannel. In this way subcooling and forced conviction inside the channel using water as cooling fluid.

2.1.24 Sidy Ndao et al. (2009)

Sidy Ndao et al. showed in the studies that multi objective approach is rather helpful then single objective approach for comparison of these cooling techniques. Because there are many variables on which these techniques depends.

2.1.25 Chen S-J and Hwang CL (2011)

Chen S-J and Hwang CL reviewed the various fuzzy and multiple attribute decision making methods and at proposed a new approach called Graph theoretic- Matrices permanent approach.

2.1.26 R. Venkata Rao

R. Venkata Rao reviewed the Graph theoretic- Matrices permanent approach and applied on manufacturing technology.

2.1.27 Adil Baykasoglu (2014)

Adil Baykasoglu reviewed the Graph theoretic – Matrix permanent decision making approach with two examples.

2.1.28 Naresh Yadav et al. (2010)

Naresh Yadav et al have applied this approach for selection of thermal plants. In this way the author considered various variables which govern the selection of power plant to compare the different power plants.

2.2 Literature review related to CFD simulation of spray cooling

Spray cooling is one of the high heat flux technique and $1000\mathrm{W}/cm^2$ is achieved by using this. Since this process cooling technique has very high heat flux that's why it will be very useful to simulate it which further results in optimization of that phenomenon. There are many sub-phenomenon encountered during the spray cooling and are difficult to model in CFD. These sub-phenomenon are described as follows

2.2.1 Langrangian approach:-

The spray cooling is done by droplets which are very high in number and every drop is traced using Langrangian approach. This is very difficult using current computational resources. Different approaches are attained by combining the droplets to do the simulation. These combinations of particles are called parcels. The number of parcels is given as an input in ANSYS Fluent and mass of each parcel is calculated by following formula.

$$Mass\ of\ each\ parcel = Mass\ flow\ rate\ of\ fluid \times \frac{lenth\ of\ time\ step}{Number\ of\ parcels} \qquad \text{Eq. 12}$$

According to CFD simulation by John M. Kuhlman et al. (2014) there were 3.69 x 10^6 parcels in the system after 5 milliseconds of simulation. This shows the number of droplets inside the system to be computed by the Langrangian approach.

2.2.2 Spray formation

Spray formation is the initial step of spray cooling in which the fluid is changed into small droplets. In this way the pressure is dropped across the nozzle and resulting in formation of sprays. There are several authors whom worked on individual modeling of this process and it further implemented in commercial softwares like Fluent or Star CCM+. Rehman et al. (2004) had done the modeling of swirling jet flow nozzle using volume of fluid method. This work was very close the Lin and Ponnappan (2003) experimental work. Tryggvason et al. (2001) classified this process into two steps. Primary breakup which is done in nozzle and secondary breakup which will further discussed in following paragraphs. In commercial softwares there are many models by which spray is generated. Like plane orifice atomizer, pressure swirl atomizer, air blast atomizer, flat fan atomizer and effervescent atomizer. Besides all these models for spray generation there are manual injection of spray is also available. There are various types of injections are available like single, group, cone, solid cone and surface. In these injections every variable of spray would be given manually. Like Sauter mean diameter (d_{32}). Since this is known that the droplet size is not uniform and there are many standard models which describes variation of size. Rosin Rammler, Rosin Rammler logarithmic are the models which are implemented in ANSYS Fluent. From them only one model

named Rosin Rammler model is used by two authors John M. Kuhlman et al. (2014) and Masoumeh Jafri (2014). Apart from these standard models Monte Carlo diameter distribution to show the variation of diameters and variation of diameters show good results with Monte Carlo method Paul Jousaf Kreitzer (2010).

2.2.3 Secondary breakup of droplets

There is work done by many authors to describe the secondary breakup of droplets. Liu Jing and Xu Xu (2009) has solved 2D Naviar Stroke equation for gas and liquid droplets and used Level Set method to find the two phase interface. The author finds the four modes of breakup: oscillation, bag breakup, sheet stripping breakup and shear breakup depending on Weber number, liquid Reynolds number, Gas Reynolds number and density ratio. According to Kékesi T. et al. (2014) which found the deformation and breakup of droplet using volume of fluid method and found out bag, shear and intermediate breakup does not depends on weber number instead of that it depends on density and viscosity. There are many models which governs the secondary breakup of droplets in ANSYS Fluent. These models are TAB, Wave, KHRD and SST. Taylor analogy breakup (TAB) is best for low weber number droplets. Wave model was given by Reitz R. D. (1987) is used for high speed injections for Weber number >100. KHRT model includes the Kelvin-Helmholtz model of breakup with aerodynamic waves and Rayleigh-Taylor model of shedding of droplets. Its use is limited to high Weber number sprays excluding low pressure sprays. SSD is Stochastic Secondary Droplet breakup model in which it is assumed that the breakup depends on discrete random event.

This phenomenon is occurs due to aerodynamic breakup of droplets. The different regimes of breakup are described below:-

S. No.	Breakup regime	Weber number
1.	Vibrational breakup	$\mathrm{We} < 12$
2.	Bag breakup	$12 < \mathrm{We} < 50$
3.	Bag and Stamen breakup	$50 < \mathrm{We} < 100$

4.	Sheet Striping	$100 < \text{We} < 350$
5.	Catastrophic breakup	$\text{We} > 350$

Table. 1 Different breakup regimes

From literature review it has been found out that KHRT model is used by two different authors John M. Kuhlman et al. (2014) and Masoumeh Jafri (2014).

2.2.4 Combining Langrangian approach with Eularian Approach

The splashing of droplet on surface has been studied by Kizito et al. (2004) and Pasandideh-Fard et al. (2001) using Tryggvason front tracking model and Volume of fluid method respectively. Former found out that maximum heat transfer take place when there is largest spreading take place. Apart from that basic work there are various models available in literature to combine the Langragian approach with Eularian approach in various commercial softwares. DPM wall film and Eularian wall film models are available in ANSYS FLUENT. Moreover Bai Gossman model is available in the case of STAR CCM+ and ANSYS CFX. Further two non-dimensional numbers named Weber number and Laplace number governs this phenomenon. The non-dimensional numbers are described as follows

I. Weber number

It is the number which relates between kinetic energy and surface tension. It is ratio of both of them and is mathematically shown below.

$$We = \frac{\rho d U}{\sigma} \qquad \text{Eq. 13}$$

Where ρ is density, d is diameter of droplet, U is normal impact velocity and σ is surface tension coefficient

II. Laplace number

This number relates between surface tension and viscous forces. This shown mathematically as

$$La = \frac{\rho d U}{\mu^2} \qquad \text{Eq. 14}$$

These numbers governs that how the droplets will behave on striking on surface. These behaviors are given by Bai et al. (2002).

I. Adhesion

When momentum of droplet is very less than the droplet will stick to the wall and coalesce completely. It is the case which happened when $We < 2630 < La^{-18}$ in the case of dry wall.

II. Rebound

In this regime the momentum of droplet is very high and it reflects back after striking with the surface. The range of weber number is less than 20 for wet wall and less than 50 for dry wall.

There are further two phenomenon occur in the case of dry wall. If Weber number is less than 80 and greater than 50 than rebound with breakup occurs and if Weber number is greater than 80 then breakup occurs.

III. Spread

The droplet strike and spread on wall film. For this phenomenon the condition is $20 < \mathrm{We} < 1320La^{-18}$for wet wall only.

IV. Splash

In this process the droplet hits the liquid layer and make a crown which further change into droplets and some part of liquid become the part of liquid layer. Splash is occurred when $\mathrm{We} > 1320La^{-18}$in the case of wet wall and $\mathrm{We} > 2630La^{-18}$in the case of dry wall. Experimentally it was determined by Moreira et al. (2010) that average Weber number for splashing is lower than actual value for splashing criteria but still splashing occurs. The reasons were not given by him. Similar thing was shown by Hillan and Kulheman (2013) that for splashing the smallest weber number to splash is between 1 and 3 while weber number for largest splashing droplets were 300 to 1000.

Since these numbers are depending on various parameters which are very difficult to measure in spray cooling like velocity of droplet, diameter of droplet. Moreover film thickness is one of the major parameter which is very difficult to measure. Taylor et al. (2014) reported the range of film thickness with time ranges between 140 microns to 180 microns. This was also justified by Pais et al. (1989) that smaller the wall thickness

higher the heat transfer rate. Apart from them the work by Pautsch et al. (2004) shows that film thickness is between 152 and 150 microns by experimental and numerical method. Sivakumar and Tropea (2002) justified the film thickness between 55 to 192 microns.

2.2.5 Turbulence in wall film

Since droplets are very high in number and when they got strike with wall film the chaotic nature of them create turbulence in wall film. This turbulence is not similar to the turbulence created by the wall shear. This turbulence is created by the impinging of droplets and apart from that the wall film models are not included turbulence in them. So it is difficult to implement these models but in literature the simulation is carried out using Standard k-Ɛ modeled is implemented to model in by John M. Kuhlman et al. (2014) and Masoumeh Jafri (2014) implemented SST K- ω model to model the spray model.

2.2.6 John M. Kuhlman et al. (2014)

John M. Kuhlman et al. (2014) there were 3.69 x 10^6 parcels in the system after 5 milliseconds of simulation.

2.2.7 John M. Kuhlman et al. (2014) a

John M. Kuhlman et al. (a) simulated the spray cooling with different wall film models using symmetry wall conditions using 90^0, 45^0 and 30^0 domains to decrease the computational time with or without energy equation. Also the author has done simulation with dual particle wall film model and Eularian wall film model. These all done step by step like in first step comparison between Dual particle wall film and Eularian wall film is done and after getting promising results with Eularian wall film model the energy equation is introduced with Eularian wall film model. Apart from standard K-Ɛ turbulence model

the Eddy viscosity model of Bossinesq is introduced to capture the turbulence due to droplet impinging with turbulence viscosity = 4μ is used to get the promising results.

2.2.8 Rehman et al. (2004)

Rehman et al. have done the modeling of swirling jet flow nozzle using volume of fluid method. In this way effect of different fluid properties by using water, FC-72, FC-77, FC-87, and methanol has simulated at different nozzle geometry. The effect of different flow rates has also been studied. The effects of these variables on pressure drop and nozzle angle have studied.

2.2.9 Murat Dinc et al. (2013)

Murat Dinc et al. have done the simulation of spray cooling without heat transfer with varying height, gravity, flow rate, spray half angle, density, viscosity and surface tension to find out the effect of these variables on spray impact efficiency. According to the author the spray efficiency increased by high gravity, viscosity, surface tension whereas the efficiency also increased by low height and low density of fluid.

2.2.10 Masoumeh Jafri (2014)

Masoumeh Jafri has simulated the spray cooling process using Star CCM+ and with water as cooling fluid and found out 8.2 to 9.1% error while calculating the heat transfer. In this way the following models included.

Phenomenon	**Model**
Turbulence	SST K-ω
Wall model	Bai Gossman model
Droplet breakup model	TAB model
Phase change	No phase change

Spray droplet size distribution	Rosin Rammler
Spray type	Solid cone spray

Table 2 Simulation parameters used by Masoumeh Jafri (2014)

2.2.11 Liu Jing and Xu Xu (2009)

Liu Jing and Xu Xu has solved 2D Naviar Stroke equation for gas and liquid droplets and used Level Set method to find the two phase interface. The author finds the four modes of breakup: oscillation, bag breakup, sheet stripping breakup and shear breakup depending on Weber number, liquid Reynolds number, Gas Reynolds number and density ratio.

2.2.12 Kékesi T. et al. (2014)

Kékesi T. et al. found the deformation and breakup of droplet using volume of fluid method and found out bag, shear and intermediate breakup does not depends on weber number instead of that it depends on density and viscosity.

2.2.13 Reitz R. D. (1987)

Reitz R. D. gives the wave model of secondary breakup of droplets which was further implemented in ANSYS Fluent and is used for high speed injections for Weber number >100. In this case the breakup is take place due to vilocity difference between two fluids and breakup caused due to higher effect of Kelvin-Halmothz instabilities.

2.2.14 Kizito et al. (2004)

Kizito et al. studied numerically and practically the splashing of droplet on surface using Tryggvason front tracking method. In this study the effect of different parameters like weber number, Reynolds number, Peclet number on spreading and splashing. The changes in these parameters have been done by changing surface tension, viscosity and thermal diffusivity. In this case low Weber number cause rebound of droplet. The decrease in Reynolds number causes

decreases the spread of the droplet. The conclusion has been made that the variables which controls the phenomenon has to be varied in small range to get high heat transfer rate

2.2.15 Pasandideh-Fard et al. (2001)

Pasandideh-Fard et al. modeled the splashing of droplet using volume of fluid method and studied the droplet splashing experimentally by varying the vilocity of droplet and temperature of the surface. In this way the study also suggest that the heat transfer increase with increase in Weber number. Besides that increase in velocity causes increase in spreading of droplet.

2.2.16 Bai et al. (2002)

Bai et al. gives the four process of droplet strike on surface depends on Weber number and Laplace number. These are Adhesion, Rebound, Spread and Splash.

2.2.17 Moreira et al. (2010)

Moreira et al. reviewed the droplet impact phenomenon and find that average Weber number for splashing is lower than actual value for splashing criteria but still splashing occurs. This happens because of liquid film and surface texture.

2.2.18 Hillan and Kulheman (2013)

Hillan and Kulheman showed that for splashing the smallest weber number to splash is between 1 and 3 while weber number for largest splashing droplets were 300 to 1000.

2.2.19 Taylor et al. (2014)

Taylor et al. reported in their studies that the range of film thickness with time ranges between 140 microns to 180 microns.

2.2.20 Pais et al. (1989)

Pais et al. studied the spray cooling using air atomizer nozzle and found out the effect of subcooling droplet size and flow rate. In this study the heat flux of 1180W/cm^2 has been achieved. The author also justified that smaller the wall thickness higher the heat transfer rate.

CHAPTER 3. Methodology

In this chapter the methodology taken during the research will be discussed. There are two section in this chapter in which first section is composed of methodology related to comparison of various cooling techniques and in the second section the methodology taken for CFD simulation of spray cooling is discussed.

3.1 Methodology for comparing the different cooling techniques

- Collect the different attributes which governs the selection process of the cooling technique.
- Classify the different attributes into different categories by thinking intuitively.
- To compare the different techniques the MADM-CCSD technique is followed. This technique is described as follows.

3.1.1 MADM-CCSD technique

In this research the author has found out many attributes which governs the selection of cooling technique for an electronic system but all these attributes does not have importance. There are some which governs during a selection process these are called pertinent attributes. Selection process using MADM-CCSD technique is described as follows.

3.1.1.1 Elimination step

First of all there is a need of fixing certain threshold value of pertinent attributes which is fixed by the help of group of experts according to the need. Then the full database of available heat exchanging techniques is searched on the basis of these threshold values. Some of them are eliminated in this search.

3.1.1.2 Formation of decision matrix and normalization

After the elimination step there is few number of candidates and attributes which are selected and in this step they are ranked according to nearest to the optimum.

In this way first all the alternative solutions are to write them in the matrix form with attributes to form decision matrix **Dn×m** in which rows comprised of **n** number of alternative solutions and columns consist of their respective values for **m** number of pertinent attributes. This matrix is non-normalized (having different dimensions for different attributes)

Decision matrix (**Dn×m)** which should be converted into normalized matrix **N n×m** (having same scale from 0 to 1) by applying following formula

$$n_{ij} = d_{ij} \Big/ \left(\sum_{i=1}^{m} d_{ij}^2\right)^{1/2} \quad \text{Eq. 15}$$

3.1.1.3 Calculation of weights using CCSD method

The calculation of weight is done in several steps which are given below

Step 1:-In this step the decision matrix (**Dn×m)** converted into normalized matrix **($Z_{n\times m}$)** by using following formulas

For cost attributes

$$z_{ij} = \frac{d_j^{max} - d_{ij}}{d_j^{max} - d_j^{min}} \text{ (i=1, 2…….n; j=1, 2 ….m)} \quad \text{Eq. 16}$$

For beneficial attributes

$$z_{ij} = \frac{d_{ij} - d_j^{min}}{d_j^{max} - d_j^{min}} \text{ (i=1, 2 ….n; j=1, 2 ….m)} \quad \text{Eq. 17}$$

Step 2:- Give initial weights ($W_{1\times m}$) in such a way that $W \geq 0$

$$\sum_{j=1}^{m} w_j, \quad j = 1,..,m \qquad \text{Eq. 18}$$

Step 3:- The overall assessment ($A_{n\times 1}$) of every alternative is calculated by

$$a_i = \sum_{j=1}^{m} z_{ij} w_j, \quad i = 1,..,n \qquad \text{Eq. 19}$$

Step 4:- Now remove the each attribute from the decision matrix and find its effect on overall assessment. This is done by removing (O_k) from the decision matrix and again calculates the overall assessment by

$$a_i = \sum_{j=1\, j\neq k}^{m} z_{ij} w_j, \quad i = 1,..,n \qquad \text{Eq. 20}$$

Step 5:- In this step the correlation coefficient ($R_{1\times m}$) is calculated with respect to (O_k) which is calculated by

$$r_j = \frac{\sum_{i=1}^{n}(z_{ij}-\bar{z})(a_{ij}-\overline{a_j})}{\sqrt{\sum_{i=1}^{n}(z-\bar{z_j})^2 \sum_{i=1}^{n}(a_{ij}-\overline{a_j})^2}} \quad \text{j=1...m} \qquad \text{Eq. 21}$$

Where $\overline{n_j} = \frac{1}{n}\sum_{i=1}^{n} z_{ij}, \quad j = 1, \ldots\ldots m,$

And $\bar{a} = \frac{1}{n}\sum_{i=1,}^{n} z_{ij} w_j, \quad j = 1, \ldots\ldots m,$

Step 6:-Now find the standard deviation by the following formula with respect to (O_k)

$$\sigma_j = \sqrt{\frac{1}{n}\sum_{i=1}^{n}\left(z_{ij} - \bar{z_j}\right)^2}, \quad j = 1, \ldots m \qquad \text{Eq. 22}$$

Step 7:- Minimize the function

$$E = \sum_{j=1}^{m} \left(w_j - \frac{\sigma_j \sqrt{1-r_j}}{\sum_{k=1}^{m} \sigma_k \sqrt{1-r_k}} \right)^2 \quad \text{Eq. 23}$$

Subject to $\sum_{j=1}^{m} w_j = 1 \, ; w_j \geq 0, \qquad j = 1, \ldots . m$

In this step to minimize the function the author used the MATLAB function which is given in the appendix of this paper and for global minimization of the function the author used multiple start random weights as input in MATLAB function. This results the global minimization of the function. The minimum of all the inputs gives the weights matrix ($W_{1\times j}$) which is used further in this paper.

The resultant of this gives the weights matrix ($W_{1\times j}$).

3.1.1.4 Formation of weighted normalized matrix

This matrix $\mathbf{M_{n\times m}}$ is obtained by multiplying columns of normalized matrix with weighted matrix. This weighted normalized matrix has all the alternative solutions with pertinent attributes along with the weight of these pertinent attributes.

3.1.1.5 Ranking of the heat exchanging technique using TOPSIS

The ranking of the techniques is done by help of TOPSIS method which is described as follows

The weighted normalized matrix used to find best and worst benchmarks which are used to find optimized technique (which is far from best and nearer to best). In this first find out the highest value from each column called best benchmark $\boldsymbol{B_m^+}$and lowest value called worst benchmark$\boldsymbol{B_m^-}$.

Then after this step find closeness of each element towards positive and negative benchmark by use of following formula in respective column.

Distance from best benchmark is given by

$$S_n^+ = \left(\sum_{j=1}^{m} \left(m_{ij} - B_j^+ \right)^2 \right)^{\frac{1}{2}} \quad \text{Eq. 24}$$

Similarly distance from worst bench mark is given by

$$S_n^- = \left(\sum_{j=1}^{m} \left(m_{ij} - B_j^- \right)^2 \right)^{\frac{1}{2}} \quad \text{Eq. 25}$$

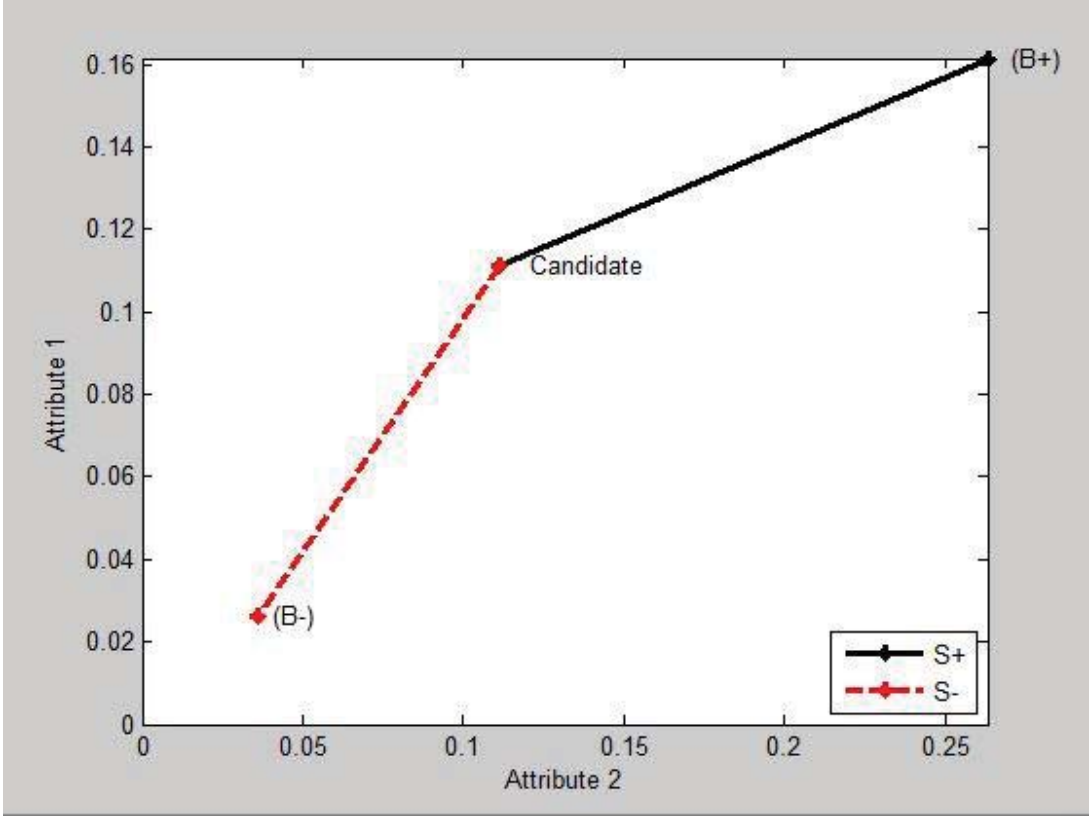

Figure 1 **Graphical representation of TOPSIS**

Then after this step find out the suitability of each alternative towards the ultimate goal is given by using S_i^+ and S_i^- to findR_i. Highest value of R_i more leads to more preferred alternative. The value of R for each alternative is given by

$$R_i = S_i^- / (S_i^+ + S_i^-) \qquad \text{Eq. 26}$$

Rank matrix is found out by arranging value of R_i in descending order which indicates most preferable at top.

The whole methodology has been shown in following figure.

3.2 Methodology taken for CFD simulation of spray

In this section the methodology taken during the research will be explained. In this way the commercial software packager ANSYS 15.0 is used to perform the simulation. The simulation is conducted in Fluent module of ANSYS 15.0. The complete steps of simulation are explained below.

3.2.1 Geometry building

This is first and foremost step of simulation in which geometrical domain to perform the simulation has been built. In this way the ANSYS Design modeler is used to build the geometry which is used for the further steps of simulation. In this way the basic dimensions of the geometric domain are matched with previous research of Murat Dinc et al. (2014) which is used as a reference for this research. The geometrical design used by Murat Dinc et al. (2014) was a cylinder having 165mm height and 152mm diameter and is shown in figure.

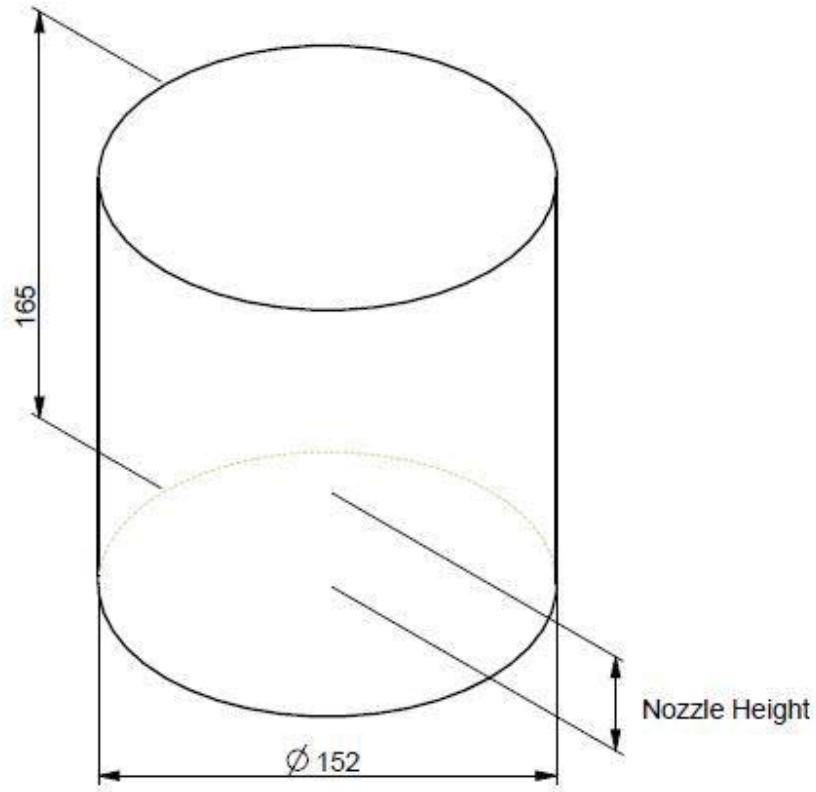

Figure 2 Geometry used by Murat Dinc et al. (2014)

Since the wall film mass dependence on spray angle and multiple nozzles is to be studied in this research the geometrical domain is modified to meet the requirements. In this way the semi cylindrical domain is made having 165mm radius and 152 mm depth. The domain is shown in figure.

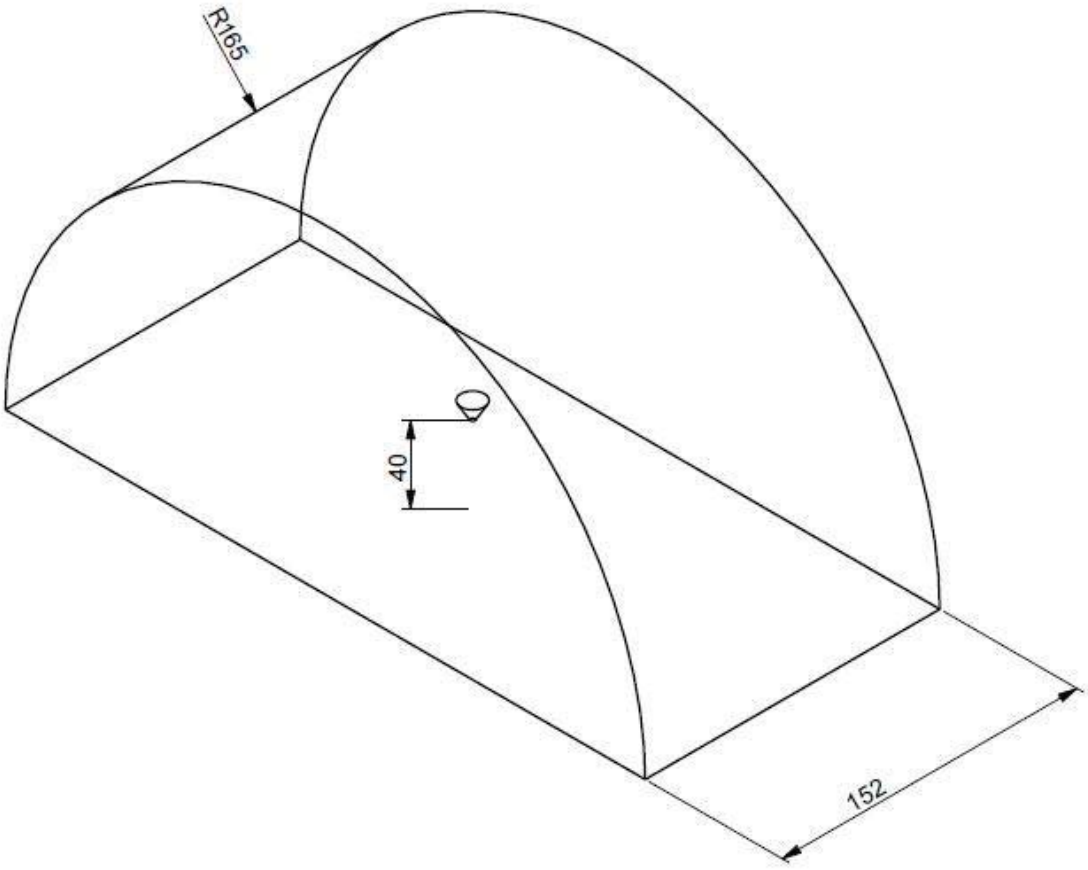

Figure 3 Geometry used in present study

In this way the change in angle cause rotation of nozzle about the center point of the spray impact circle and which is handled by circular shape of the domain. Further the multiple numbers of nozzles (up to 4) are also handled by this domain.

3.2.2 Mesh Generation

The mesh is generated in the Mesh module of ANSYS 15.0. In this way three different meshes were generated having 72444, 241264 and 1085317 elements. In this way grid independence test was conducted using three different meshes. The result of wall film mass was compared at 6 milliseconds and the wall film mass were 3.983312, 4.213352 and 4.214231 mg for three different meshes starting from

coarser to finer mesh. There is very less change in wall film mass was taken place from 241264 to 1085317 elements mesh was taken place. In this way 241264 elements mesh was used in further analysis process. The three meshes are shown in figure.

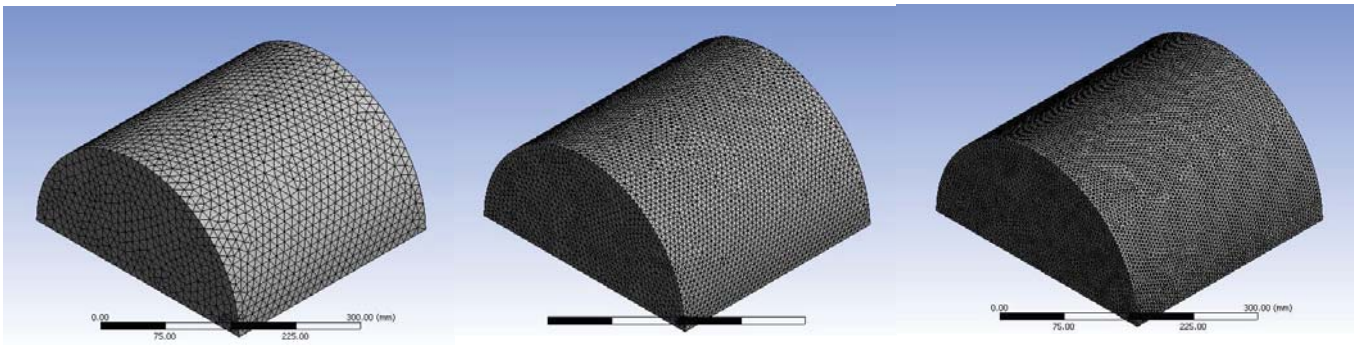

Figure 4:- 72444, 241264 and 1085317 elements mesh respectively from left to right.

In this way boundary inflation was used to capture the thin wall film and turbulence in thin wall film on the impact surface of domain while meshing. There are 20 layers of boundary inflation was taken having 1 micron first layer and growth rate of 1.2. The boundary inflation was used in all three meshes which are used for grid independence test. The boundary inflation is shown in figure.

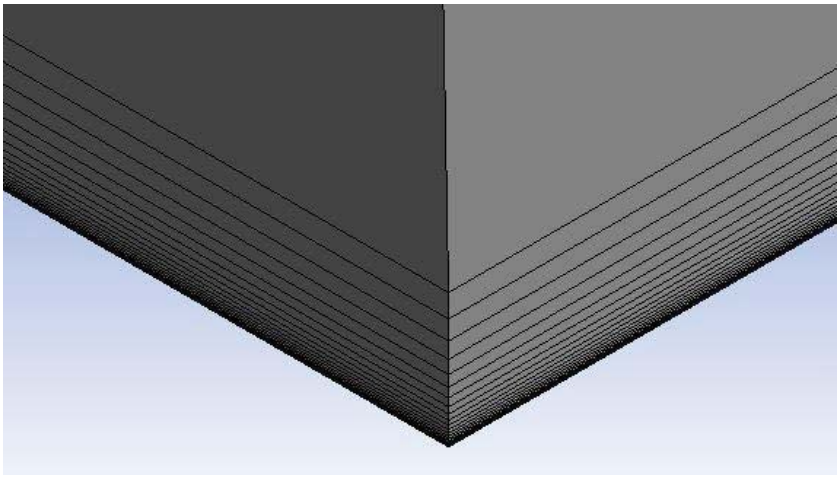

Figure 5 Boundary inflation

The skewness properties of 241264 elements mesh are shown in following table.

Minimum skewness	Maximum skewness	Avg. skewness	Standard deviation
1.32072289572571E-05	0.792432519830485	0.197525464796468	0.113312504937467

Table 3 Mesh properties

3.2.3 Numerical modeling

While thinking about the numerical modeling of spray cooling there is following different physical models to be required to consider in the case of spray on a flat plate.

- Spray formation
- Tracking of spray particles
- Capturing turbulence due to droplet movement in air and droplet impact on impact wall
- Gravitational force
- Continues injection of particles in the domain
- Wall film formation

To implement all the above factors into the numerical modeling the following models are used in ANSYS Fluent module.

The DPM (Discrete phase modeling) is used to inject spray particles of water into air domain. DPM is a combination of Euler approach as well as Langrangian approach in which particles of sprayed water is tracked using Langrangian approach in continues phase of air. Number of continues phase iterations per DPM iteration is a key factor to successful convergence of solution. In this way higher the continuous phase iterations per DPM iterations leads to larger time to converge the solution but more stable residuals. In other words higher number of continues phase iterations gives larger number of iterations to continuous phase to converge per DPM iteration which cause disturbance in continuous phase. Normally its value varies from 10 to 30. In this way 20 number of continues phase iterations are set per DPM

iteration. In DPM the particles are injected using pressure swirl atomizer model. The other parameters of pressure swirl atomizer injection are shown below

Upstream pressure	Height of nozzle	Spray axis	Flow rate	Spray half angle
10^6 Pascal	40mm	-y	.003 Kg/Sec	10°

Table 4 Injection properties

In this way the number of particle streams injected per DPM injection is further optimized to get better results with less particles injection (more the number of particles higher time taken during DPM iterations). Number of particle streams is the number of parcels injected in the system. Parcel is the combination of multiple numbers of droplets. In this way mass of each parcel is given below.

$$Mass\ of\ each\ parcel = Mass\ flow\ rate\ of\ fluid \times \frac{lenth\ of\ time\ step}{Number\ of\ parcels} \quad \text{Eq. 27}$$

In this way continues injection is done with continuous phase time step which is defined to be .0001 sec. Maximum number of steps till which a particle to be tracked is also optimized which will discussed in next paragraphs of this chapter. Higher the number of steps leads to higher chances of particle to be trapped in a loop in continues phase. Moreover the length of time step is a key factor which is defined as the time step after which the equation of motion of particle again calculated. Its value set to be 5 in this research work.

Further the droplet breakup models have been used to capture aerodynamic breakup of droplets. In this way there are many models to capture this breakup like TAB, Wave, KHRD and SST. Taylor analogy breakup (TAB) is best for low weber number droplets. Wave model was given by Reitz R. D. (1987) is used for high speed injections for Weber number >100. KHRT model includes the Kelvin-Helmholtz model of breakup with aerodynamic waves and Rayleigh-Taylor model of

shedding of droplets. Its use is limited to high Weber number sprays excluding low pressure sprays. SSD is Stochastic Secondary Droplet breakup model in which it is assumed that the breakup depends on discrete random event.

This phenomenon is occurs due to aerodynamic breakup of droplets. The different regimes of breakup are described below:-

S. No.	**Breakup regime**	**Weber number**
1.	Vibrational breakup	$We < 12$
2.	Bag breakup	$12 < We < 50$
3.	Bag and Stamen breakup	$50 < We < 100$
4.	Sheet Striping	$100 < We < 350$
5.	Catastrophic breakup	$We > 350$

Table 5 Different breakup regimes

In this way KHRT model is been used in this research to capture the secondary breakup of droplets.

The effect of gravity on spray droplets and wall film is considered in this research. The acceleration due to gravity is set 9.81 in negative Y direction. In this way the body force of gravity is used in momentum equation.

To implementing continues injection of particles into the system the transient model has to be used. In this way the time step of .0001 is used for continuous phase iterations and the same time step is used to injecting the mass into the system. In this way the simulation of the system is done till 6 ms.

The turbulence is created in the continuous phase while droplets travel through the continuous phase and also when droplet strikes on wall film. Since droplets are very high in number and when they got strike with wall film the chaotic nature of them create turbulence in wall film. This turbulence is not similar to the turbulence created by the wall shear. This turbulence is created by the impinging of droplets and wall film models are not included turbulence in them. So it is difficult to implement these models but in literature the simulation is carried out using Standard k-Ɛ modeled is implemented to model in by John M. Kuhlman et al. (2014) and Masoumeh Jafri (2014) implemented SST K- ω model to model the spray cooling. To capture the turbulence, K-Ɛ model is used which was used previously by Murat Dinc et al. (2014).

The phenomenon of formation of wall film is conversion of Langrangian approach to Eularian approach. In this way there are two different models to capture the physics. In this way Eularian wall film model and DPM wall film model are two models to capture the film formation. In this research author used both of them to validate the results and the DPM model gives good validation with previous literature. In this way the DPM model is further used in the research.

3.2.4 Optimization of number of parcels

In the case of spray the numbers of droplets are very high and it is difficult for computational resources to track that much higher number. This problem is handled by combining the droplets into parcels. Lower the number of parcels leads to less computational time but inaccurate results and vice versa. In this way there are different number of parcels are injected per unit time step and the results are compared with previous literature. This results in optimization of number of parcels with less DPM iteration time. The results for different number of parcels are shown below with mass accumulated in wall film after 6 ms.

Number of parcels injected per time step	**Wall film mass at 6 ms**	**Time taken for iteration of last time step**

1000	3.911201 mg	1 minute
5000	4.023653 mg	1.5 minutes
10000	4.213352 mg	2.5 minutes
30000	4.213781 mg	63 minutes

Table 6 Optimization of number of particles

In this way 1000 numbers of parcels are used for further simulation.

3.2.5 Validation of results

In this case the wall film mass is compared with the previous results with vertically downward spray having mass flow rate .003 Kg/Sec and spray height 40mm with same nozzle as used by Murat Dinc et al. (2014). The comparison of results is shown in following graph.

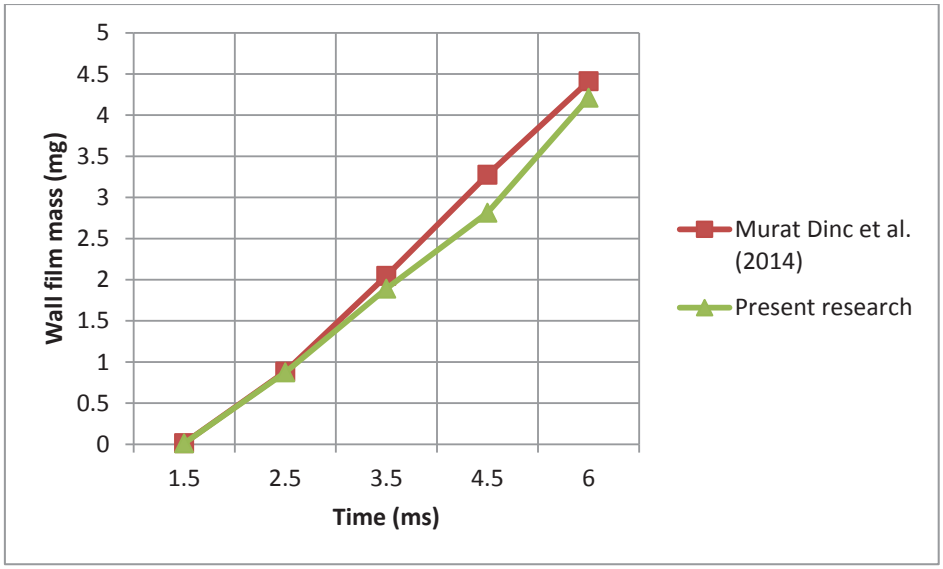

Figure 6 Graph of comparison of two studies

In this way the percentage error come in the results is shown in following graph

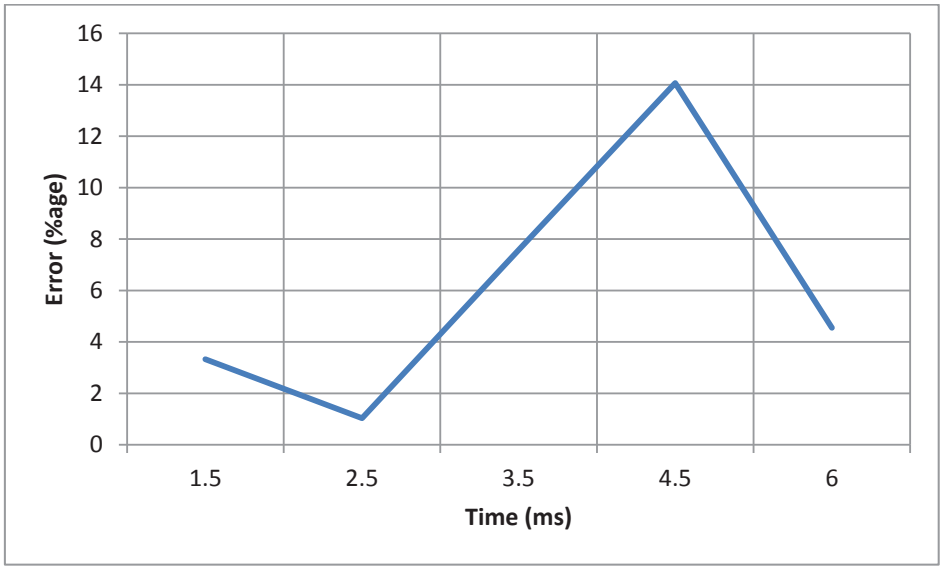

Figure 7 Graph of relative error (%age)

3.2.6 Strategy for changing spray variables

In this research the different variable like spray angle, number of spray nozzles, distance between multiple spray nozzles have been modified. This is discussed in following paragraphs

3.2.6.1 Change in spray angle

The nozzle inclination with negative Y axis is changed. The simulation is done by inclining the nozzle at 15°, 45° and 75° with negative Y axis. The arrangement of nozzles is shown in following figure 8.

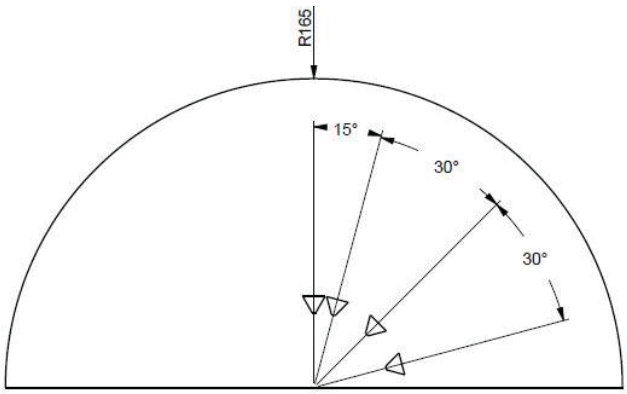

Figure 8 Different nozzle angles

3.2.6.2 Change in number of nozzles

In this case the numbers of nozzles are increased. This is done by taking the same pressure drop but equally dividing the mass flow rate in all nozzles. In this way the 2, 3 and 4 nozzles are taken into account for spray simulation.

3.2.6.3 Change in distance between nozzles

In this way the distances between above taken nozzles have been varied. The different number of nozzles (2, 3 and 4) are taken at different distances. The distances between nozzles are takes as 10mm, 26mm and 42mm. In this way total nine numbers of cases are taken under simulation. These nine cases are shown in following table

Case	Number of nozzles	Distance between nozzles
1	2	10mm
2	2	26mm
3	2	42mm
4	3	10mm
5	3	26mm
6	3	42mm
7	4	10mm
8	4	26mm
9	4	42mm

Table 7 Different cases taken for study

The arrangement of nozzles with distance is shown in following diagrams

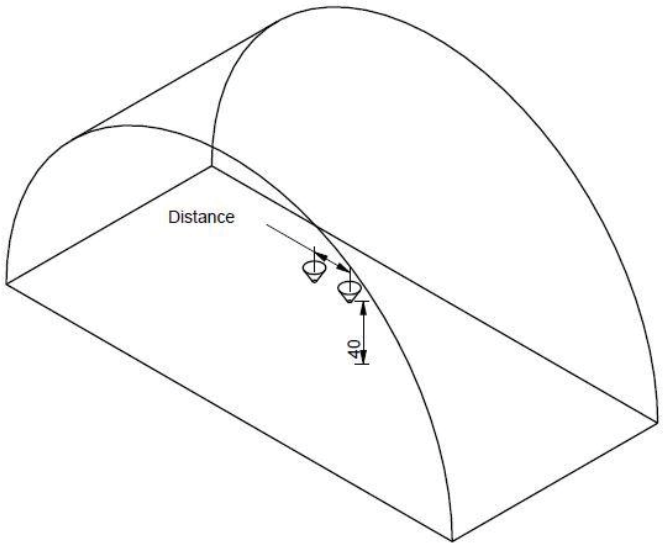

Figure 9 Two nozzles arrangement

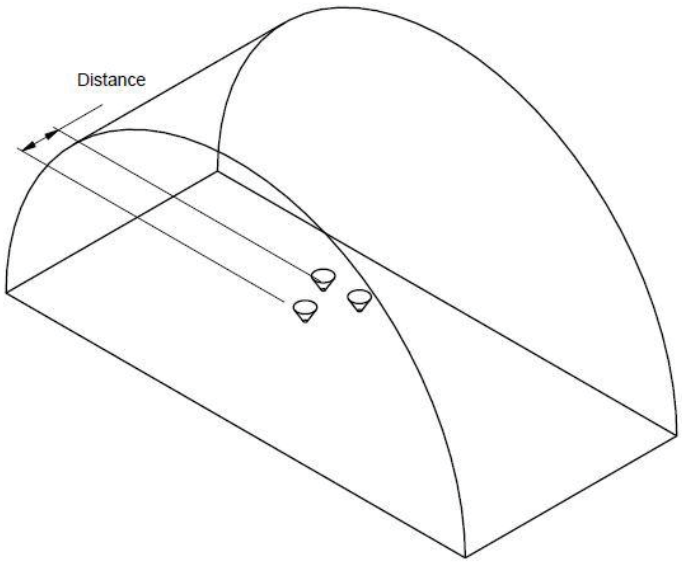

Figure 10 Arrangement of three nozzles

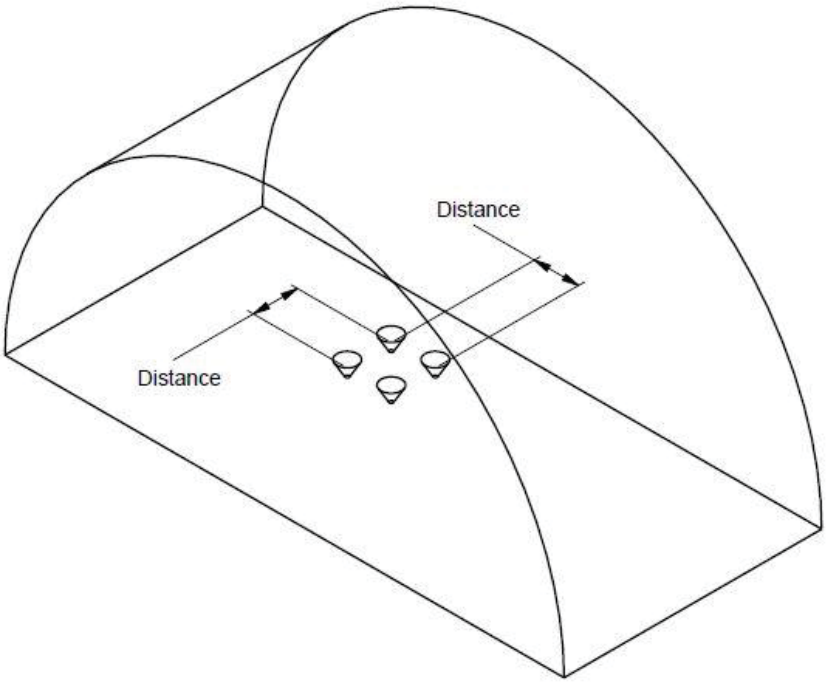

Figure 11 Arrangement of 4 nozzles

CHAPTER 4. Results and discussions

In this chapter the results came from the research are discussed in details. In this way in first section of this chapter the results related to the research which is done on comparison of various cooling techniques is discussed and this section is further divided into two parts. The first part is classification of various attributes on which the selection of cooling technique depends is discussed and in the next part the comparison of cooling techniques has been done.

Further in the second section of this chapter the results related to CFD simulation of spray cooling in which the wall film mass in different conditions have been discussed.

4.1 Comparison of cooling techniques

4.1.1 Classification of attributes

From the literature review the author has found out there are many attributes which governs the selection of cooling technique. These attributes are first divided into two major groups.

- Attributes specific to each technique.
- General attributes.

The purpose of this division is to nullify the effect of specific characters of each cooling technique on overall selection process for example the nozzle diameter cannot be used in the case of microchannel which is specific character of spray cooling technique. Moreover the specific characters are helpful in comparing the different experiments of that specific technique so that the best one should be used in overall selection process. Besides that the specific attributes of each technique gives an idea about how many attributes governs that technique and will helpful to design the experiments so that effect of each attribute on performance of technique can be quantified. This is shown in **table**

The specific attributes further divided into four groups

- Heat transfer rate
- Flow rate

- Pressure drop
- Miscellaneous factors

First three groups are the performance characters and the attributes governs these characters are grouped in respective group and the other attributes which governs the technique are grouped in fourth group. This type of grouping is done because high heat transfer rate is required with low flow rate and low pressure drop. Furthermore the addition of cost and manufacturing groups is possible which are not added now due to deficiency of data.

The general attributes on which the comparison of different techniques is done, are divided into five groups

- Performance
- Overall size of device
- Fluid used
- Reliability
- Miscellaneous factors

The performance group contains the performance attributes which is major expectation from any technique and the overall size of device group contains all attributes which affect the space required to implement the technique because as the miniaturization of electronics products increases this aspect is very important. The third group is of coolant fluid properties which are used in all the cooling techniques and this is put into general attributes category because this is not specific to each technique. Reliability is the major aspect which has to be accomplished for uninterrupted working of the system and in the case of cooling techniques there are major problems of fouling and clogging. The last group is of miscellaneous factors which indirectly or directly affect the overall comparison of cooling techniques. The general attributes also used for comparison in each specific technique but reverse is not possible.

4.1.2 Quantification of attributes

Each of the above attribute can be quantified on the basis of experimental data which is available in the previous literature. From that data one can develop the whole database for every attribute like pressure drop 900 kilopascal, flow rate .2 liter/min etc. Some attributes which are either yes or no like delicacy of device which come into picture only in jet impinging technique and one can give these factors either 0 or 1. Some attributes which are not quantifiable and these can be quantified according to the extent or probability by the help of experts like incipience temperature drop factor is more in the case of dielectric fluids.

4.1.3 Coding scheme

The attributes which are found out and are classified as explained above are shown in Table 2. There are two types of coding approaches used by author. One is overall coding of all techniques which is applicable to all techniques and is based on general attributes and another one is the coding specific to each technique. In the case of specific coding scheme there is one code which is given for each technique ((A) for single phase microchannel flow cooling, (B) for two phase microchannel flow cooling, (C) for jet cooling and (D) for spray cooling) and the codes after that is specific to that technique. This series is further expanded for other cooling techniques which are not included in this research work like miniature loop heat pipe, compact thermosyphon etc. Furthermore there are different numbers of codes which are specific to each technique depending on number of attributes on which that technique depends. Like single phase microchannel flow cooling has 14 attributes and there are 14 codes which are specific to this technique which comes after code A. Prior to specific coding scheme there comes the general coding scheme in which all general attributes are codify. These codes are illustrated in Table 3. The codes 1 to 23 in general attributes category are in serial order as shown in Table 2 and one code from A, B, C and D is given for each specific category and next to that 1 to 25 are the codes given for each specific category. In this research work author considered only four cooling techniques and among them 25 is the maximum

number of attributes given for each specific category and these codes vary for each cooling technique according to number of attributes governing them.

General attributes	1	2	3	4	5	6	7	8	9	10	11	12	13	14	15	16	17	18	19	20	21	22	23		
Code for specific technique	A, B, C or D																								
Specific code	1	2	3	4	5	6	7	8	9	10	11	12	13	14	15	16	17	18	19	20	21	22	23	24	25

Table 8 Coding scheme

Range of heat transfer rate	**Code**
Not mention	0
1-100	1
100-200	2
200-300	3
300-400	4
400-500	5
500-600	6
600-700	7
700-800	8
800-900	9
900-1000	10
>1000	11

Table 9 Example of coding of heat transfer rate

The coding for each attribute is depend on many factors like

- Range coding is coding in which specific character is given for specific range of the attribute, like in the case of heat transfer rate attribute This range is of any type like flow rate, nozzle angle etc.
- Code specific to first letter of the attribute. Like in the case of shape of fin attribute the code T is given for triangle shape and C is given for circle and so on.
- Code specific to Yes or NO like Y is given if incipience temperature drop is there and N is given if incipience temperature drop is not there.

This coding scheme will help for standardization of experiments by codify the experimental inputs and outputs for building the database which will give the whole information about the experiment in systematic manner. In this way the experimentalist will know that which attributes are required to be considered to codify the whole experiment and moreover if every experimentalist follows this coding scheme will help to build the complete database of each and every experiment. This will help for future researchers to find out easily the areas where scarcity of data is there and conduct the experiment with similar attributes.

This coding scheme will also helpful for designers to easily find out the cooling technique required for their design because by using this coding scheme the computerized database is buildable and which will help to write computer program (described in section 5) to find out cooling scheme.

4.1.4 Comparison of cooling techniques

The step by step explanation of comparison of cooling technique is discussed as under.

4.1.4.1 Elimination step

From the literature review the author has eliminated four different experiments for each cooling technique (single phase microchannel cooling, two phase microchannel cooling, jet impinging cooling and spray cooling) and chooses four pertinent attributes which are maximum heat transfer rate, pressure drop, heat transfer coefficient and volume flow rate. These values are shown in table 6.1.1 to 6.1.4

4.1.4.2 Formation of decision matrix and normalization

Now comparison of different studies of single phase microchannel flow cooling is done using Table 5 from which the Decision matrix ($\mathbf{D_{m\times n}}$) is derived in which the rows are different alternatives and the columns are different attributes. There are 4 alternatives equal to **m** and 4 attributes equal to **n** are taken of each category for comparison.

$$\mathbf{D_{m\times n}} = \begin{bmatrix} 181 & 110 & 9.10 & .282 \\ 428 & 258 & 12.5 & 1.1 \\ 58.33 & 57.2 & 2.03 & .159 \\ 141 & 10.8 & 2.17 & 1.002 \end{bmatrix} \qquad (d_{ij} \text{ is the jth attribute of ith technique}) \qquad \text{Eq. 28}$$

Normalization matrix is derived from ($\mathbf{D_{m\times n}}$) matrix using eq. 5.2.1 and the normalized matrix is given as

$$\text{Normalized matrix } (\mathbf{N_{m\times n}}) = \begin{bmatrix} .3701 & .3840 & .5776 & .1852 \\ .8751 & .9007 & .7942 & .7224 \\ .1193 & .1997 & .1290 & .1044 \\ .2883 & .0377 & .1379 & .6580 \end{bmatrix} \qquad \text{Eq. 29}$$

Where m is number of alternatives and n is number of attributes.

4.1.4.3 Calculation of weights using CCSD method

Using the above given formulation in section 5 part 3 and by help of MATLAB function matfunc.m which is given in appendix and this function is multiple start using 10 random points as input in this function for global optimization. The resulting and minimum weights comes out from this function is given as ($\mathbf{W_{1\times n}}$) in which **n** is number of attributes.

$$\mathbf{W_{1\times n} = [0.2421 \quad 0.4304 \quad 0.0672 \quad 0.2603]} \qquad \text{Eq. 30}$$

4.1.4.4 Formation of weighted normalized matrix

Weighted normalized matrix is the resultant of both decision matrix and weighted matrix and is calculated as explained in section 5 part 4 the resulted weighted normalized matrix is ($\mathbf{M_{n\times m}}$) where **m** is number of attributes and **n** is number of alternatives

The weighted normalized matrix ($\mathbf{M_{n\times m}}$) = $\begin{bmatrix} .0896 & .1653 & .0388 & .0482 \\ .2118 & .3876 & .0534 & .1880 \\ .0289 & .0859 & .0087 & .0272 \\ .0698 & .0162 & .0093 & .1713 \end{bmatrix}$ Eq. 31

4.1.4.5 Ranking of the single phase microchannel flow cooling technique using TOPSIS

This is done by TOPSIS method which is explained in section 5 parts 5 and author calculated from each column called best benchmark $\boldsymbol{B_m^+}$and lowest value called worst benchmark$\boldsymbol{B_m^-}$. Which are calculated and written below

$\boldsymbol{B_m^-}$**= [0.0289 0.0162 0.0087 0.0272]** Eq. 32

And

$\boldsymbol{B_m^+}$**= [0.2118 0.3876 0.0534 0.1880]** Eq. 33

and the Distance from best benchmark ($\boldsymbol{S_n^+}$)is given by

$\boldsymbol{S_n^+} = [\ \mathbf{0.2901} \quad \mathbf{0} \quad \mathbf{0.3903} \quad \mathbf{0.4004}]^{\mathbf{T}}$ Eq. 34

Similarly distance from worst benchmark ($\boldsymbol{S_n^-}$) is given by

$\boldsymbol{S_n^-} = [\ \mathbf{0.1651} \quad \mathbf{0.4464} \quad \mathbf{0.0697} \quad \mathbf{0.1498}]^{\mathbf{T}}$ Eq. 35

Now the rank matrix **($\mathbf{R_n}$)** is calculated as explained is.

$\mathbf{R_{n(single\ phase\ microchannel\ flow)}}$**= [0.3627 1.0000 0.1515 0.2722]** $^{\mathbf{T}}$ Eq. 36

Now this rank is for single phase microchannel flow cooling from which the technique 2 is best parameters of which will used for global comparison between all the techniques. The whole methodology is explained in the flow chart.

4.1.4.6 Ranking of the jet impinging cooling technique

Similar to this formulation the comparison of Jet impinging cooling technique is compared and the ranking matrix is shown as

$$\mathbf{R_{n(Jet\ impinging\ cooling)}=[\ 0.0196\quad 0.1465\quad 1.0000\quad 0.1272]^T} \qquad \text{Eq. 37}$$

In this way the technique 3 is higher in this category and it will included in overall comparison

4.1.4.7 Ranking of the two phase microchannel flow cooling technique

Again the ranking of two phase microchannel flow cooling is done and the ranking matrix is given as

$$\mathbf{R_{n(Two\ phase\ flow\ cooling)}=[\ 0.5218\quad 0.4170\quad 0.2700\quad 0.6041\ ]^T} \qquad \text{Eq. 38}$$

In this way the technique 4 is higher in this category and it will included in overall comparison

4.1.4.8 Ranking of the spray cooling technique

Again the ranking of spray cooling is done and the ranking matrix is given as

$$\mathbf{R_{n(Spray\ cooling)}=[\ 0.4232\quad 0.5927\quad 0.2407\quad 0.1914]^T} \qquad \text{Eq. 39}$$

In this way the technique 2 is higher in this category and it will included in overall comparison

4.1.4.9 Overall comparison

Now the best of different techniques are found out and these best are again compared to get overall best technique. This is shown in table 6.9.1

The ranking matrix resulting from above comparison is

$$\mathbf{R_{n(Overall)}=[\ 0.2185\quad 0.9148\quad 0.0665\quad 0.2260]^T} \qquad \text{Eq. 40}$$

4.1.5 Results

In the above given methodology and comparing the four different techniques it is found out that there is not only a single property on basis of which the heat transfer techniques are compared but there are many

properties on which comparison and selection depends. Even in the selection from different experiments of same technique requires the multiple attributes to be compared. From the comparison of the four techniques it is found that jet impinging technique is better from all other three techniques on the basis of available experimental data. The comparison results are Jet impinging technique>Spray cooling>Single phase microchannel flow cooling>Two phase microchannel flow cooling. Only performance attributes and general attributes are included in this research on the basis of which above results comes out but manufacturing and costing attributes are still to be included which are not included due to deficiency of data.

4.1.6 SWOT analysis

In the given methodology the weights for each attribute is calculated. These weights are also helpful for SWOT analysis of the design of heat exchanging technique. In this way the user has to focus on weakest attributes, whose value of weight is higher. Similarly the technique having very lowest value of higher weighted attribute is the threat. In this way the experimentalist have an opportunity to increase the value of threated attribute so that the threat is decreased and finally higher value of high weighted attribute is the strength of that heat exchanging technique.

4.2 CFD simulation of spray cooling

In this section of the chapter the results of CFD simulation of spray will be discussed. In this way as discussed previously the effect of change of spray angle and increase of number of nozzles with varying distance between nozzles on wall film mass has been studied. This section is further divided into subsections in which the effect of various parameters has been discussed.

4.2.1 Effect of change of spray angle

To study this effect the spray is injected into the domain at three different angles. Apart from them the angle 0° with vertical is also compared and is used for validation with previous studies. These angles are 15°, 45° and 75° with vertical. The wall film mass is compared because higher the wall film mass

absorbed as boundary layer higher will be the heat transfer rate. In this way it increases the absorption efficiency. The wall film mass and the absorption efficiency is shown in following graph

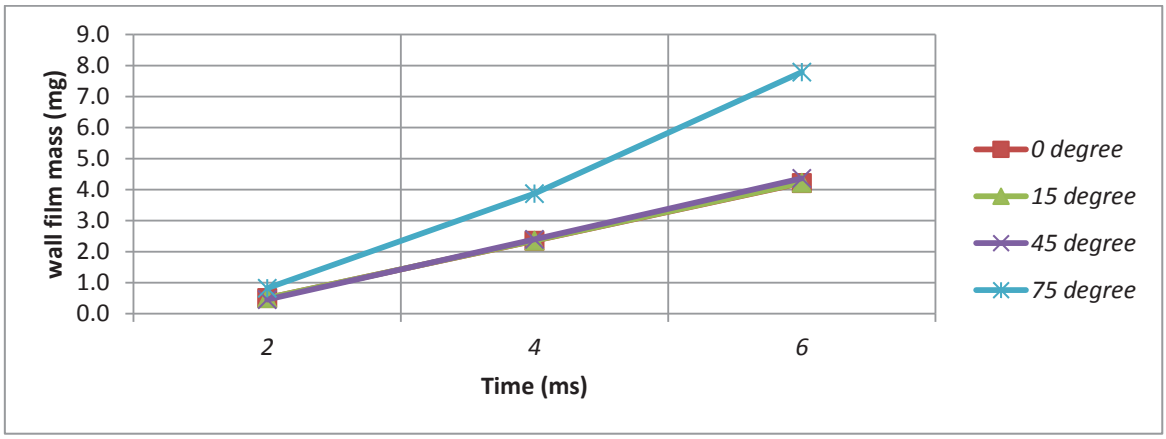

Figure 12Variation of wall film mass with time with different angles of nozzle

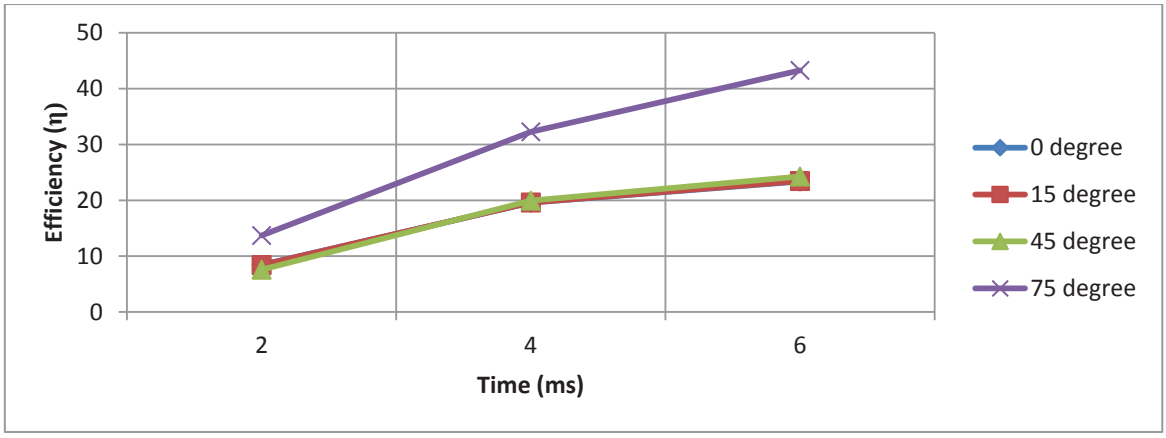

Figure 13 Variation of efficiency with time step with different angles of nozzle

From the graph it has been interpreted that as the angle of nozzle with vertical increases the wall film mass accumulation increases which leads to increase in absorption efficiency. This scenario changes abruptly as the angle changes from 45 degree to 75 degree. From the velocity diagram it is observed that the rebounded droplets which are near to nozzle come again in contact of upcoming spray droplets and again fall back on surface but this phenomenon does not happen in the case of 15 degree with vertical because in that case the inclination is high.

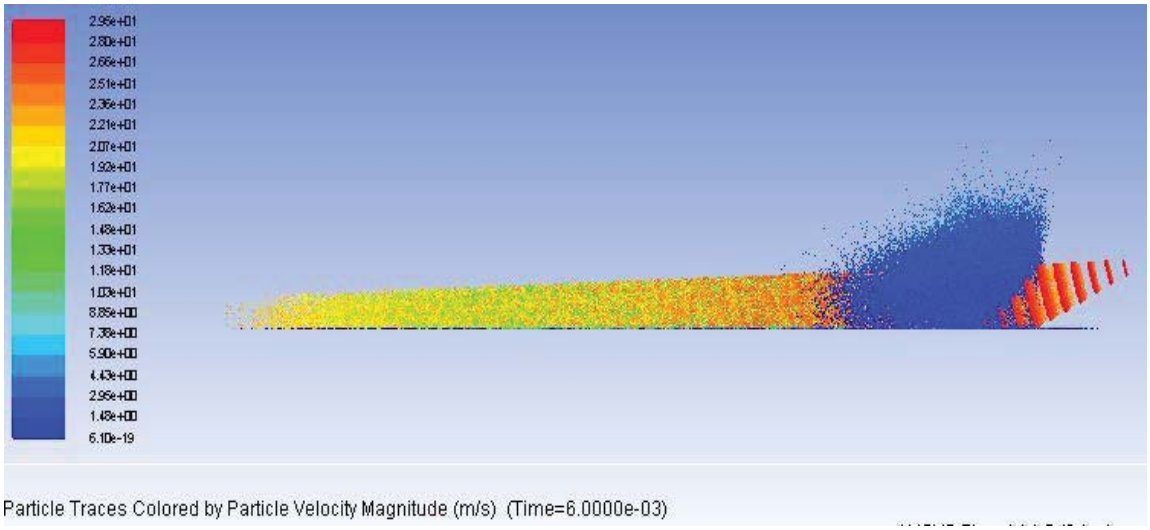

Figure 14 Particle vilocity contour at 75 degree nozzle angle

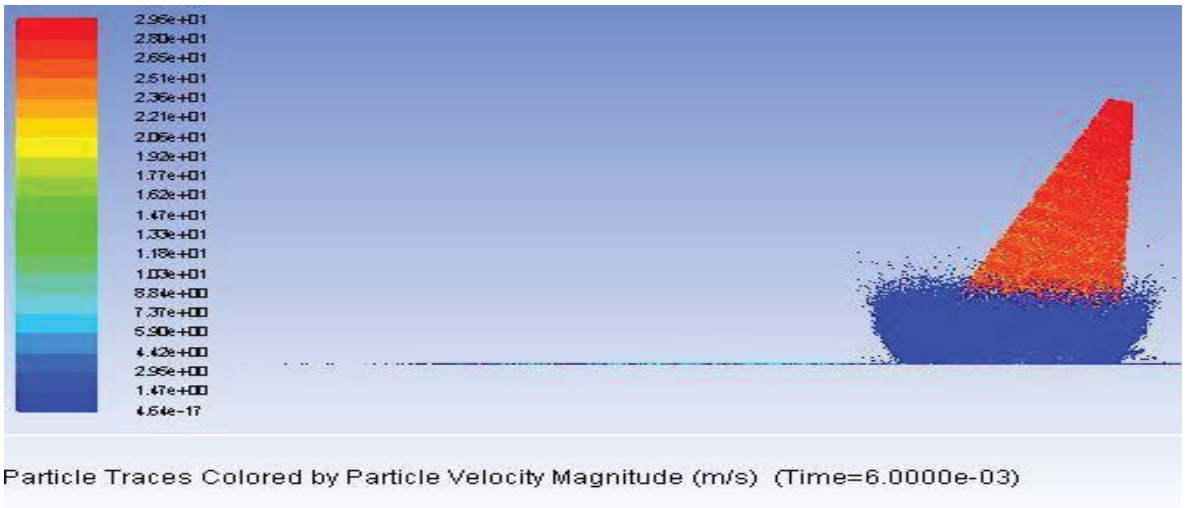

Figure 15 Particle vilocity contour at 15 degree nozzle angle

Further the maximum wall film height of the four cases is shown in following graph.

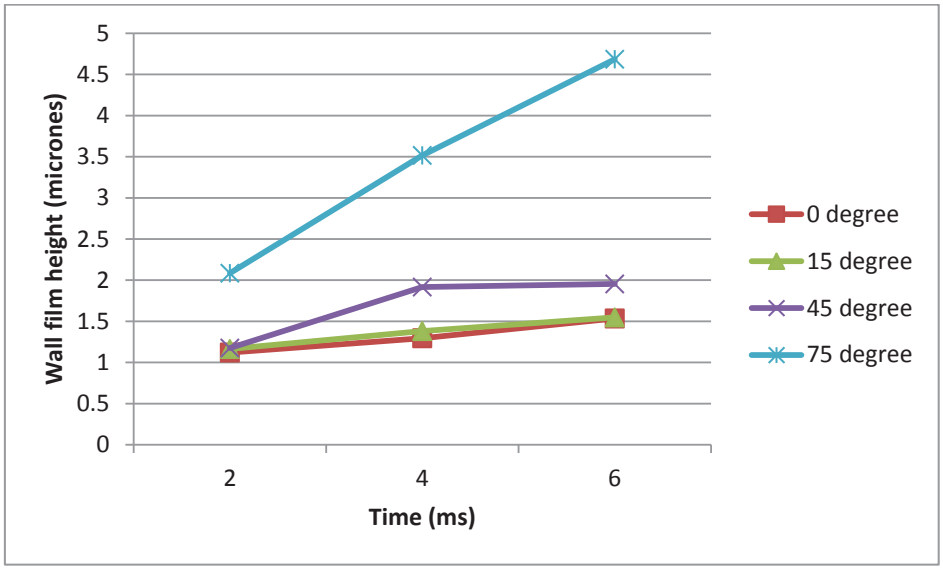

Figure 16 Variation of wall film height with time at different nozzle angles

This graph shows that as the time increases the film height also increase but on the other side the film height also increases with increase in angle with vertical. This is because the film mass increases which lead to increase in film height. This also advocates the increase in absorption efficiency which will lead to increase in heat transfer rate. This is also shown in following film height diagrams of four cases at 60ms

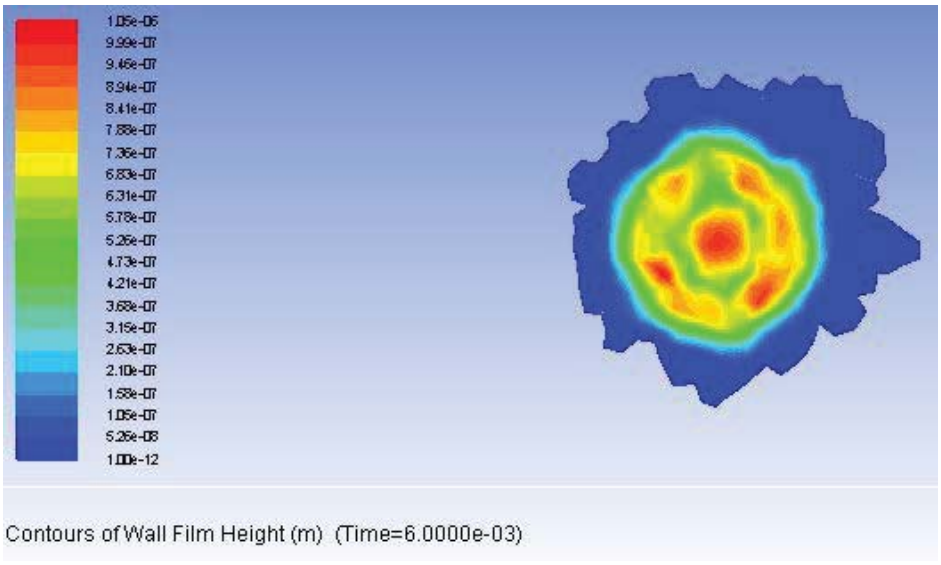

Figure 17 Contours of wall film height with 0 degree angle with vertical

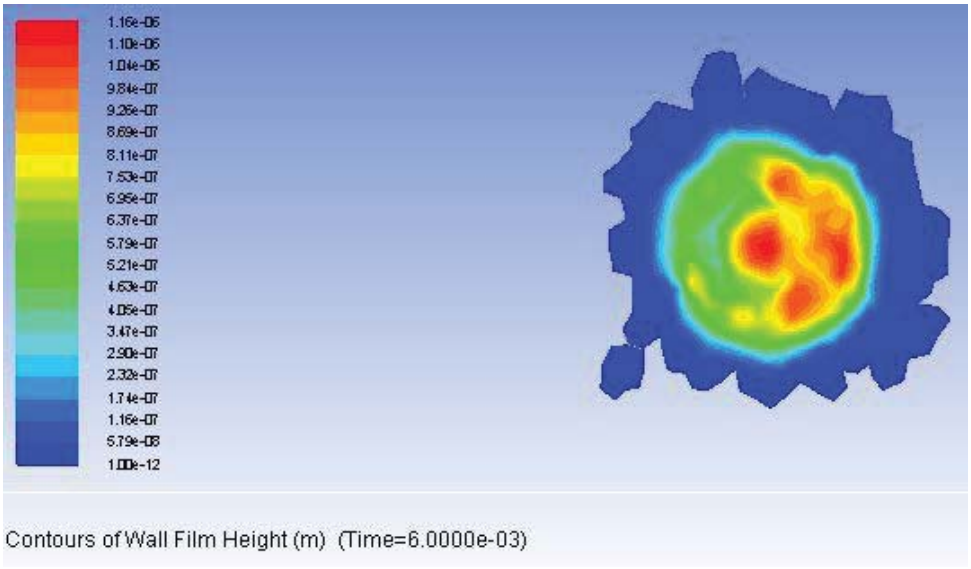

Figure 18 Contours of wall film height with 15 degree angle with vertical

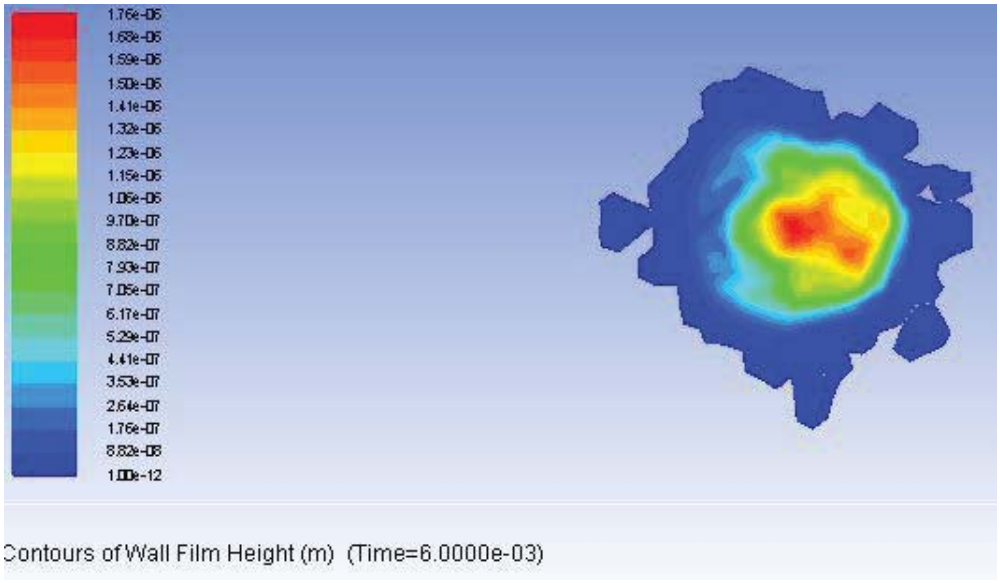

Figure 19 Contours of wall film height with 30 degree angle with vertical

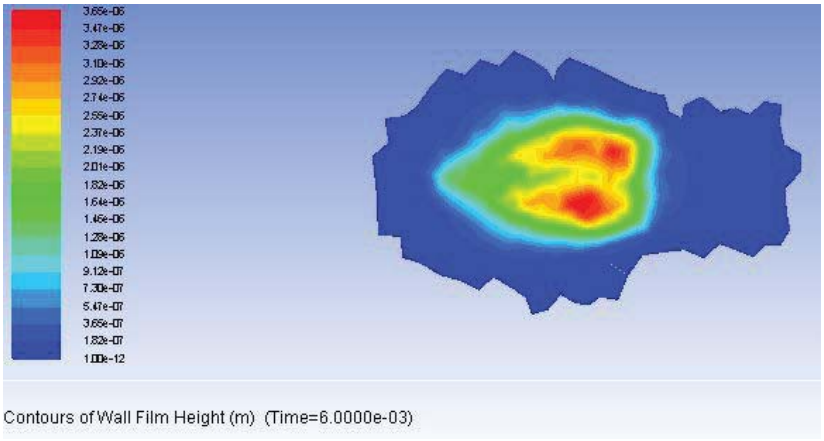

Figure 20 Contours of wall film height with 75 degree angle with vertical

In this way in the case of 75 degree the spread is more in comparison to other cases which leads to high heat transfer in spray cooling. This is because in the case of spray cooling the wall film is required to be low and uniform.

Similarly the velocity of wall film is shown at 60ms in following diagrams.

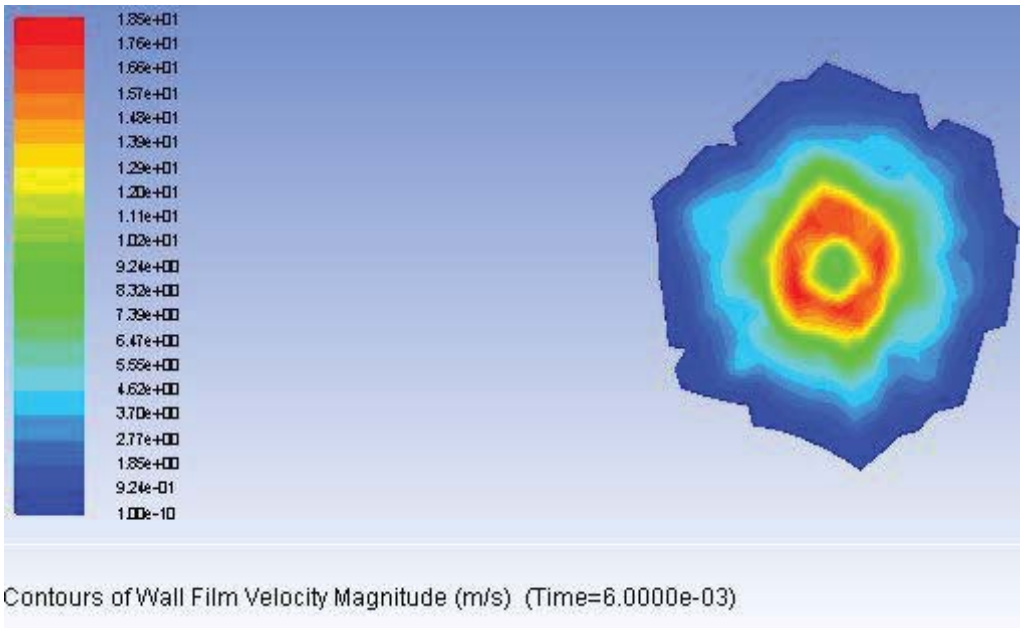

Figure 21 Contour of wall film velocity at 0 degree nozzle angle

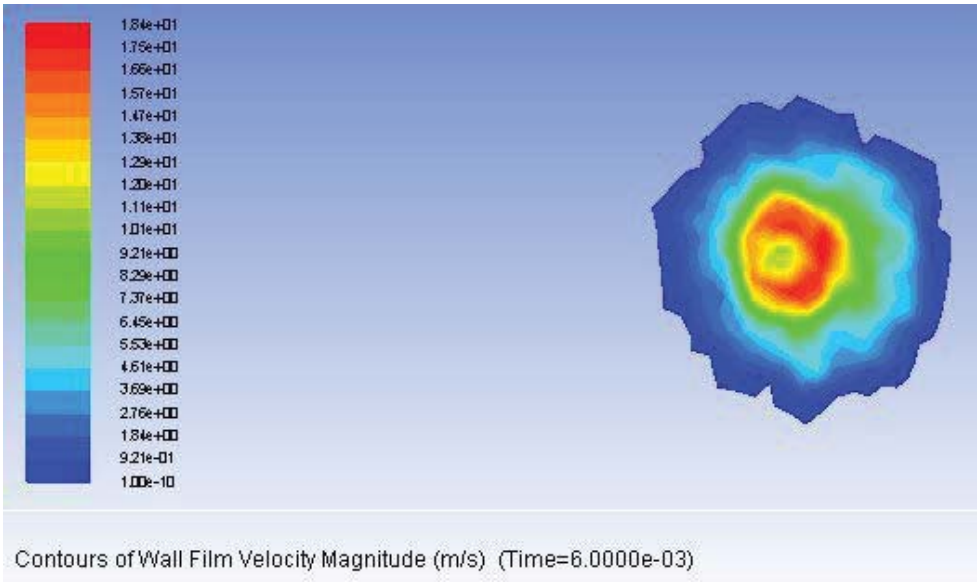

Figure 22Contour of wall film velocity at15 degree nozzle angle

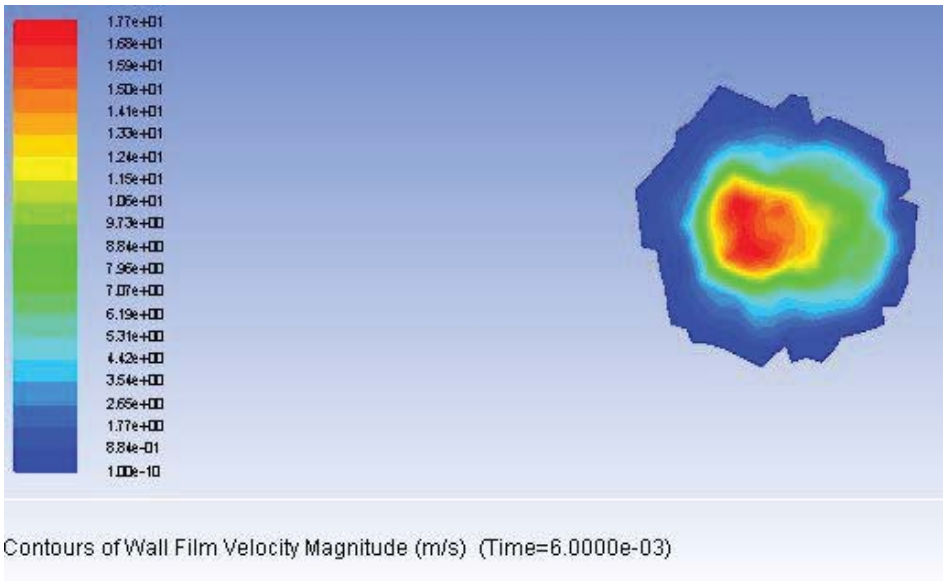

Figure 23Contour of wall film velocity at 45 degree nozzle angle

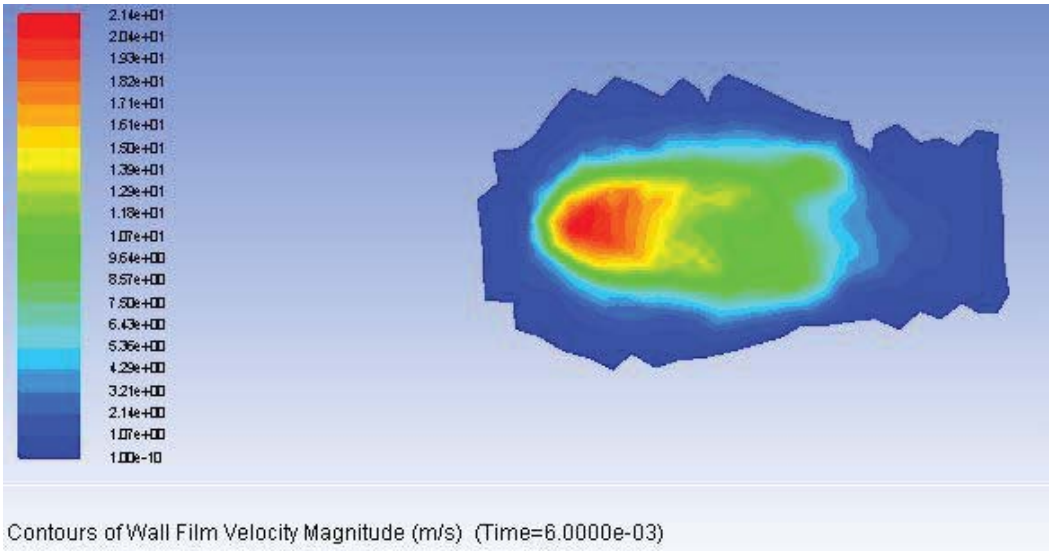

Figure 24Contour of wall film velocity at 75 degree nozzle angle

In this way it has been observed that as the angle is increased the velocity of wall film parallel to the spray axis is high this is because the moving force is provided by upcoming spray particles. Further the area covered by the wall film is higher in the case of higher angles with vertical.

4.2.2 Effect of number of nozzles with varying distance between nozzles

The effect of increase in number of nozzles is discussed in section of the chapter. In this way multiple numbers of nozzles are taken to find the effect on different parameters of spray with varying distances between nozzles. In this way the combined effect of both of the parameters on wall film mass shown in following graph

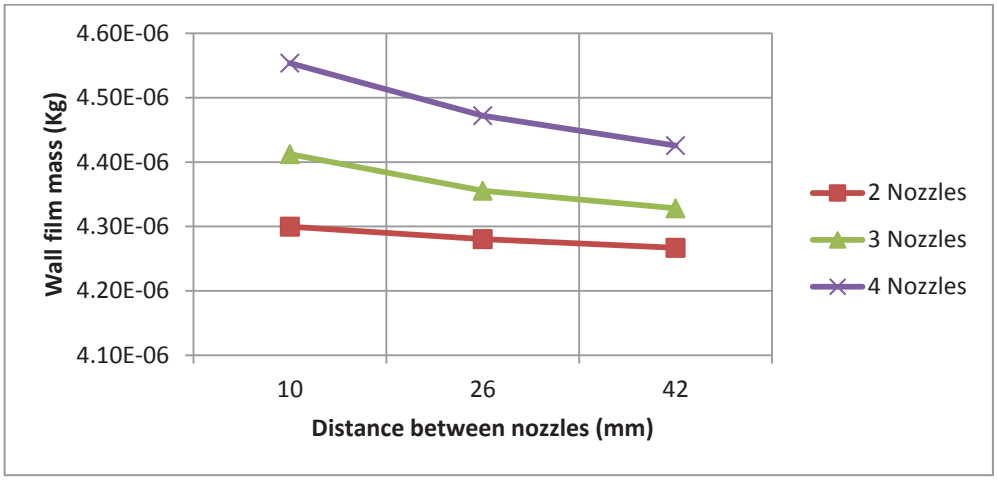

Figure 25Variation of wall film mass with distance between nozzles and different numbers of nozzles

In this way the increase in distance between nozzles leads to decrease in wall film mass. This is because as the distance between nozzles is increased the overlapping area decreased. Overlapping area of spray leads to comeback of bounced back droplets by striking in upcoming fluid. Further if the results is compared between numbers of nozzles it has been found out that the wall film mass increased by increase in number of nozzles. This is because as the number of nozzles increased the area under the spray increases and spray got more area which leads to increase in splashing. In this way it has been found out that as the number of nozzles increased the wall film mass of spray increases while on the other hand as the distance between nozzles decreased the wall film mass increases.

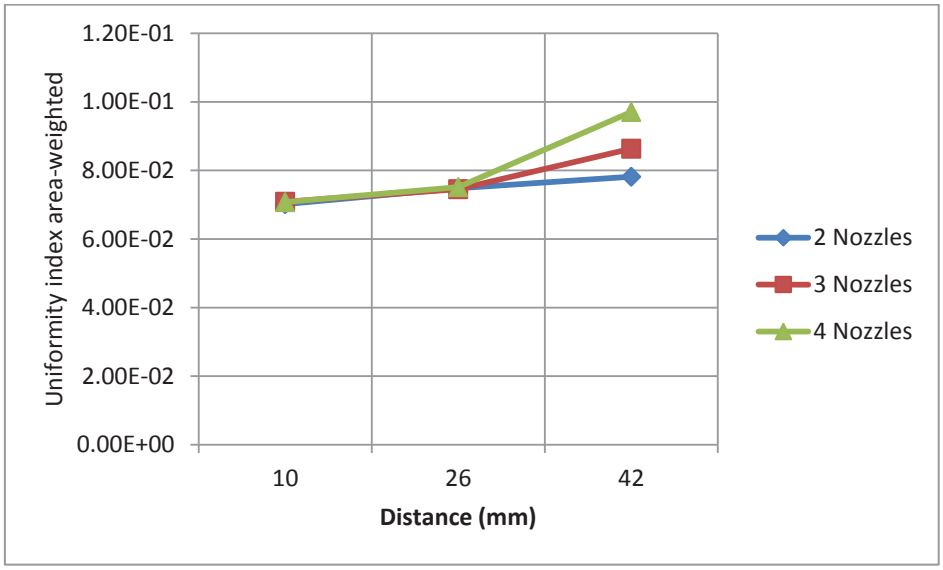

Figure 26Variation of Uniformity index with distance between nozzles and different numbers of nozzles

The above graph shows the uniformity index area weighted of wall film. In this way the uniformity index of wall film increases with increase in number of nozzles and it also increases with increase in distance between nozzles. This is beneficial in the case of spray cooling because leads to uniform cooling of the heated surface and besides that it decreases the wall film thickness which increases the heat transfer rate. This is shown in contours which are given in annexure of this research. Further the maximum film thickness is compared in the following graph.

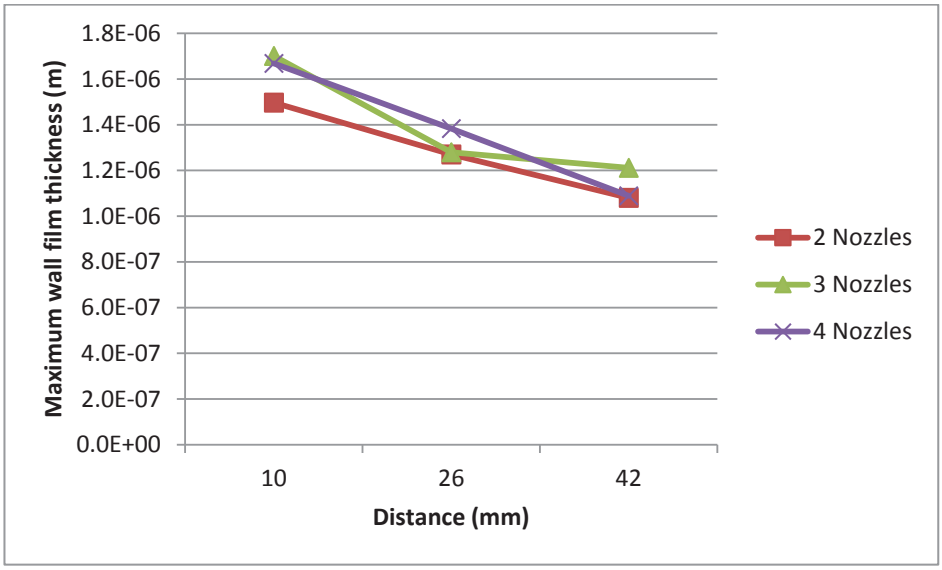

Figure 27 Variation of wall film thickness with distance between nozzles and different numbers of nozzles

In this way the film thickness shows similar trend as of mass accumulated on the impact surface increases which increases the wall film thickness. In this trend there is variation in trend in the case on 3 nozzles which are at 42mm distance apart.

The Sauter mean diameter of spray in different cases are shown in following diagrams

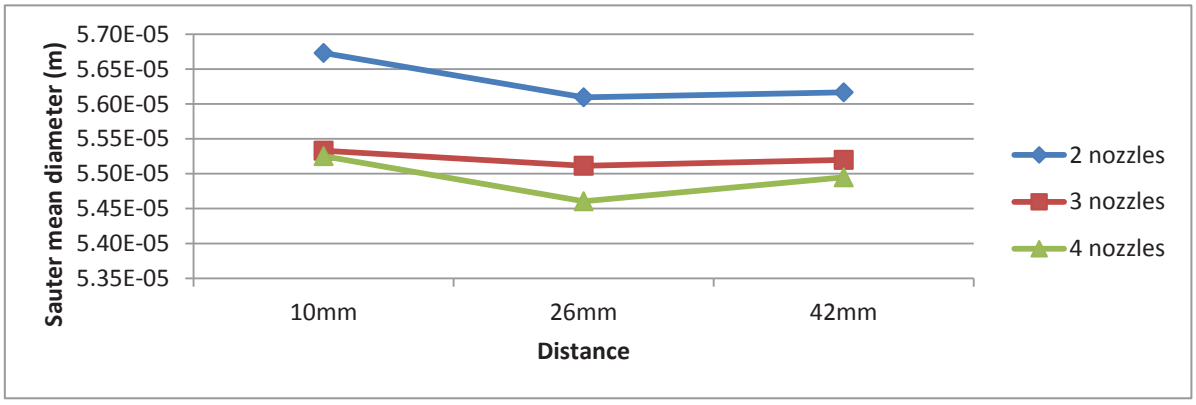

Figure 28 Graph of variation of Sauter mean diameter with distance and different number of nozzles at 2ms

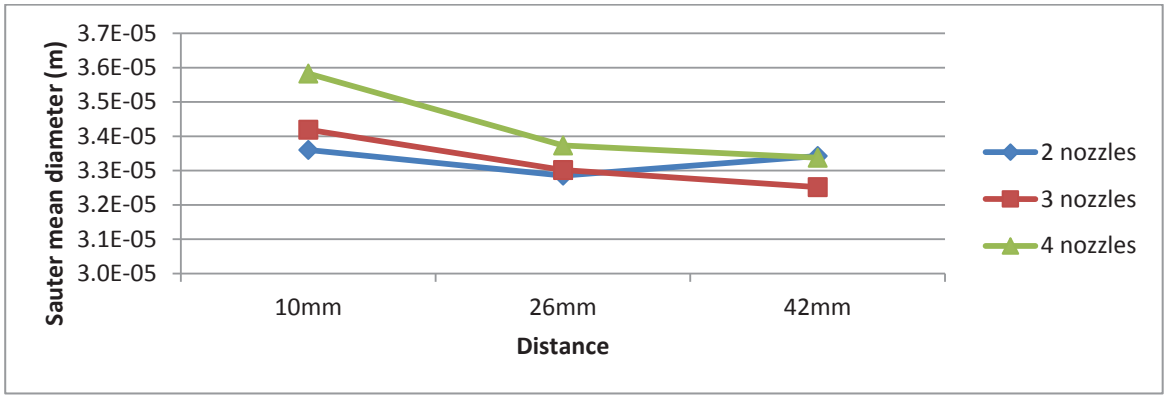

Figure 29Graph of variation of Sauter mean diameter with distance and different number of nozzles at 4ms

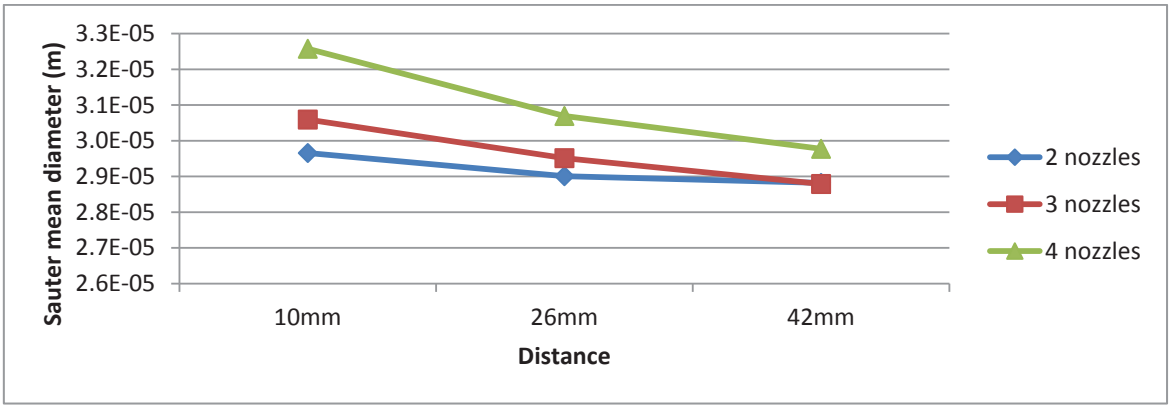

Figure 30Graph of variation of Sauter mean diameter with distance and different number of nozzles at 6ms

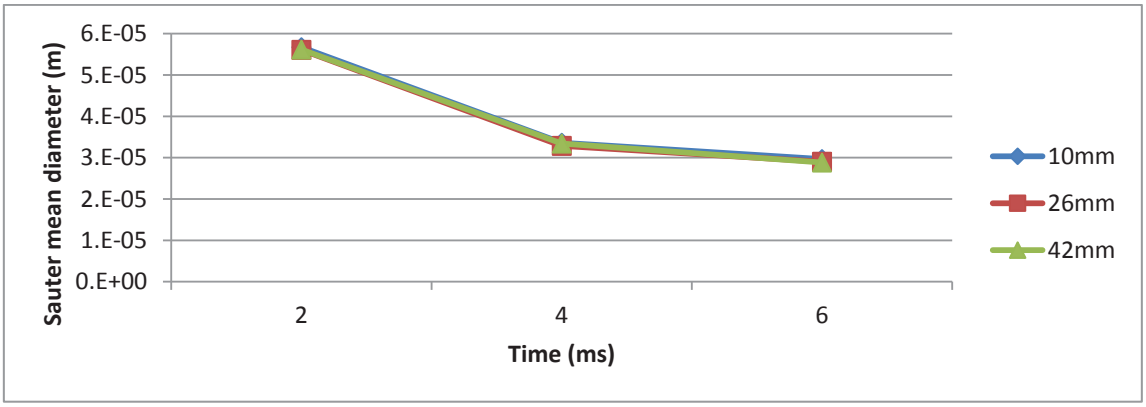

Figure 31 Variation of Sauter mean diameter with time and distance with 2 nozzles

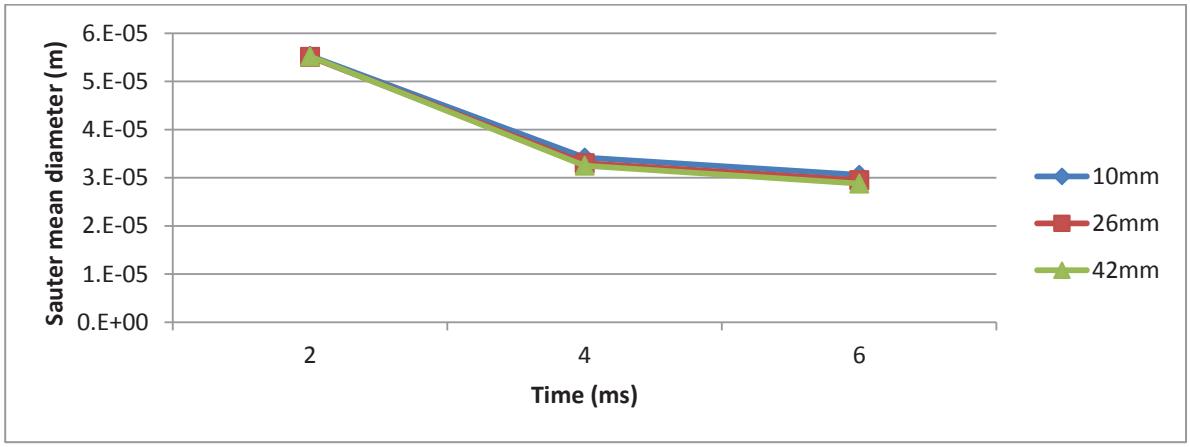

Figure 32 Variation of Sauter mean diameter with time and distance with 3 nozzles

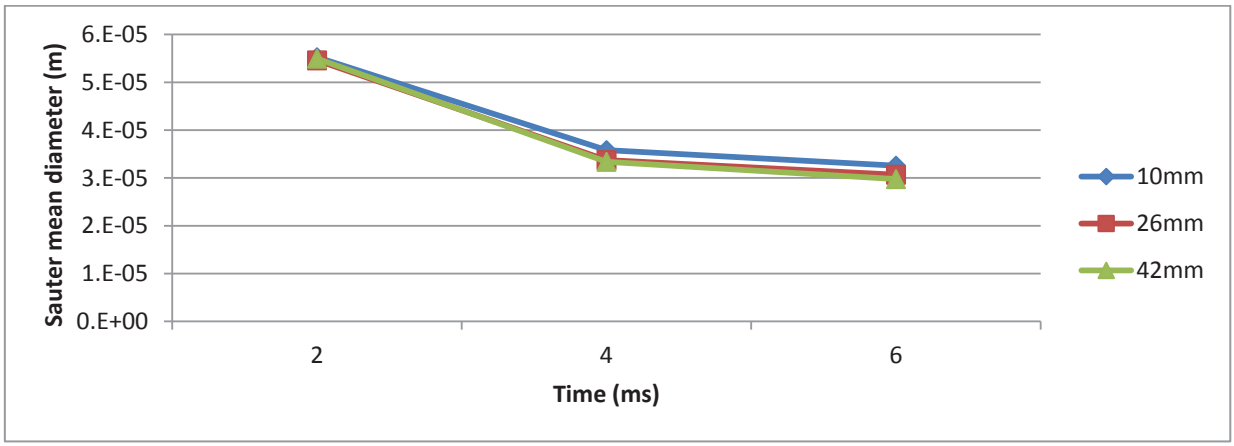

Figure 33 Variation of Sauter mean diameter with time and distance with 4 nozzles

In this way from above graphs it is inferred that as the distance between nozzles increases the Sauter mean diameter first decreases at 26mm then increases in the case all type of nozzles in case of 2ms and in the case of 2 nozzles at 4ms. In all other cases the Sauter mean diameter continuously decreases with time increase in distance and also decrease with increase in time. The Sauter mean diameter decrease with time because the spray droplets break on striking with surface and with this phenomenon average diameter of the spray decreases.

CHAPTER 5. Conclusion

In this chapter the conclusion of this research is discussed. There are two different sections of this chapter. In first section the conclusion drawn from comparison of different cooling techniques is discussed and in next section the conclusion of CFD simulation of spray cooling is discussed.

5.1 Conclusion of comparison of spray cooling

In this way the following conclusions are drawn

- The attributes on which selection of cooling technique for computer chips are collected and codified and classified into two broad categories i.e. General attributes and Specific attributes.
- The 16 different experiments of Spray cooling, Jet impinging cooling, Single phase microchannel flow cooling and Two phase microchannel flow cooling (four in each category) have been compared from which jet impinging cooling method is best one. This comparison is done on the basis of current experimental data.

5.2 Conclusion of CFD simulation of spray cooling

- By increase in time the wall film height and wall film mass increases.
- On increasing the spray angle with vertical the wall film mass has been increased. This also leads to increase in wall film height.
- Increase in number of nozzles leads to increase in wall film mass as well as wall film height.
- Increase In distance between nozzles leads to decrease in wall film mass.
- Increase in number of nozzles also increases the uniformity index of wall film.
- Increase in distance between nozzles also leads to uniformity index in wall film.
- Sauter mean diameter decreases with increase in time step.
- In the case of 2 ms the Sauter mean diameter decreases from 10mm to 26mm then again increases at 42mm in the case of all nozzles. The similar trend is shown in the case of 2 nozzles at 4 ms In all other cases the Sauter mean diameter decrease with increase in distance between nozzles.

CHAPTER 6. References

1. A.L.N.Moreira, A.S.Moita, M.R.Pana,"Advances and challenges in explaining fuel spray impingement : How much of single droplet impact research is useful?," Progress in Energy and Combustion Science, Vol. 36, pp. 554–580, 1020.
2. Adil Baykasoglu," A review and analysis of "graph theoretical-matrix permanent" approach to decision making with example applications," Artif Intell Rev, Vol. 42, pp. 573–605, 2014.
3. ANSYS Fluent User's Manual, Version 15.0, 2013.
4. Bai, C., Rusche, H., Gosman, A.,"Modeling of gasoline spray impingement", Atomization and Sprays, Vol. 12, pp. 1-27, 2002.
5. Cader T., Westra L.J., Eden R.C., "Spray cooling thermal management for increased device reliability." IEEE Transactions on Device and Materials Reliability, Vol. 4 (4), pp. 605–613, 2004
6. Charles R. Ortloff, Marlin Vogel, "Spray Cooling Heat Transfer- Test and CFD Analysis," Semiconductor Thermal Measurement and Management Symposium, pp. 245 – 252, March 2011.
7. Chen S-J, Hwang CL,"Fuzzy multiple attribute decision making: methods and applications," Springer-Verlag, Berlin and New York, ISBN 3540549986, 1992.
8. D.P. Singh, Abhishake Chaudhary, Vijayant Maan, "Selection of Heat Exchanger for Heat Operation by Multiple Attribute Decision Making (MADM) Approach," International Journal of Engineering Research & Technology (IJERT), ISSN: 2278-0181, Vol. 2 Issue 10, pp. 3072-3080, October – 2013.
9. Dan Faukner, Mehdy Khotan, and Reza Shekarriz," Practical Design of a 1000 W/cmz Cooling System," 19th IEEE SEMI-THERM Symposium.
10. Issam Mudawar, "Assessment of High-Heat-Flux Thermal Management Schemes," IEEE

Transactions on Components and Packaging Technologies, Vol. 24, No. 2, pp. 122-141, June 2001.

11. J. Stephen Taylor, John M. Kuhlman, Donald D. Gray, Murat Dinc, Krishna T. Medam, and Nicholas L. Hillen, “Techniques to quantify dynamic phenomena of spray droplets impinging on a smooth surface”, 89th Annual Meeting of the West Virginia Academy of Science, Shepherd, WV, April 12, 2014.
12. John M. Kuhlman, Donald D. Gray, Murat Dinc, Nicholas L. Hillen, Krishna Teja Medam and J. Stephen Taylor, “Spray Cooling Heat Transfer Mechanisms,” Final Technical Report on NASA Award Number NNX10AN04A, 2014.
13. John M. Kuhlman, Nicholas L. Hillen, J. Stephen Taylor, Krishna Medam, Murat Dinc, and Donald D. Gray, “Time-varying liquid volume beneath single droplet impacts into a static liquid”, 39th Annual AIAA Dayton-Cincinnati Aerospace Sciences Symposium (DCASS), Dayton, Ohio, March 5, 2014.
14. John R. Thome, “Boiling in microchannels: a review of experiment and theory,” International Journal of Heat and Fluid Flow, vol. 25, pp. 128–139, 2004.
15. Jungho Kim, “Spray cooling heat transfer: The state of the art,” International Journal of Heat and Fluid Flow, Vol. 28, pp. 753–767
16. Kizito J.P., Vander Wal R.L., Berger G.M., Iwan J., Alexander D. and Gretar Tryggvason, ”Numerical and Experimental Studies of Splashing Droplets, AIAA-2004-0960,” 42th AIAA Aerospace Science Meeting and Exhibit, 2004.
17. Lin L. and Ponnappan R., “Heat transfer characteristics of spray cooling in a closed loop”, International Journal of Heat & Mass Transfer, Vol. 46, pp. 3737-3746, 2003
18. Liu Jing, Xu Xu,” Direct Numerical Simulation of Secondary Breakup of Liquid

Drops," Chinese Journal of Aeronautics, Vol. 23, pp. 153-161, 2010.

19. Masoumeh Jafri, "Analysis of heat transfer in spray cooling systems using numerical simulations," University of Windsor, 2014.
20. Mehrdad Alemi, Hossein Jalalifar, Gholamreza Kamali and Mansour Kalbasi, "A prediction to the best artificial lift method selection on the basis of TOPSIS model," Journal of Petroleum and Gas Engineering Vol. 1(1), pp 009-015, March 2010.
21. Milan Visaria, Issam Mudawar, "Application of Two-Phase Spray Cooling for Thermal Management of Electronic Devices," IEEE Transactions On Components And Packaging Technologies, Vol. 32, No. 4, pp. 784-793, December 2009.
22. Naresh Yadav, I.A. Khan, and Sandeep Grover," Operational- Economics Based Evaluation And Selection of A Power Plant Using Graph Theoretic Approach," International Scholarly and Scientific Research & Innovation, Vol.4 (3), 2010.
23. Nicholas Hillen and John M. Kuhlman, "Characterization of sprays impinging onto an unheated surface for spray cooling applications", AIAA 38th Annual Dayton-Cincinnati Aerospace Sciences Symposium (DCASS), Dayton, OH, March 6, 2013.
24. P.P. Bhangle, V.P. Agrawal, S.K. Saha, "Attribute based specification, comparison and selection of a robot," Mechanism and Machine Theory, vol. 39, pp.1345-1366, 2004.
25. Pais M. R., Chow L. C. and Mahefkey E. T., "Surface roughness and its effect on the heat transfer mechanism in spray cooling", Journal of Heat Transfer, Vol. 114, pp. 211-219, 1992.
26. Pais M., Tilton D., Chow L., and Mahefky E., "High heat flux, low superheat evaporative spray cooling," Proceedings of the 27th AIAA Aerospace Sciences Meeting, Reno, NV, 1989.
27. Pasandideh-Fard M., Aziz S.D., Chandra S. and Mostaghimi J., "Cooling Effectieness

of Water Drop Impinging on Hot Surface," Int, J. Heat Mass Transfer, Vol. 22, pp. 201-210, 2001.

28. Pautsch A.G., Shedd T.A., and Nellis G.F., "Thickness Measurements of the Thin Film in Spray Evaporative Cooling," Inter Society Conference on Thermal Phenomena, pp. 70-76, 2004.
29. R. D. Reitz.,"Mechanisms of Atomization Processes in High-Pressure Vaporizing Sprays, " Atomization and Spray Technology, Vol. 3, pp. 309-337, 1987.
30. R. R. Schmidt, B. D. Notohardjono," High-end server low temperature cooling," Ibm J. Res. & Dev., Vol. 46, No. 6, November 2002.
31. R. Venkata Rao," Decision Making in the Manufacturing Environment Using Graph Theory and Fuzzy Multiple Attribute Decision Making Methods," Springer Series in Advanced Manufacturing ISSN 1860-5168, ISBN 978-1-84628-818-0
32. Rehman M.M., Mead. R.H., Hong C.T, Lin L., Ponnapan R.,"Numerical Analysis of a Spray Nozzle for Predictions of Cone Angle and Pressure Drop," Proceedings of the 2nd International Energy Conversion Engineering Conference, Rhode Island, 2004.
33. Satish C. Mohapatra and Daniel Loikits, "Advances in Liquid Coolant Technologies for Electronics Cooling," IEEE Advances in Liquid Coolant Technologies, Vol. 21.
34. Satish G. Kandlikar and Akhilesh V. Bapat, "Evaluation of Jet Impingement, Spray and Microchannel Chip Cooling Options for High Heat Flux Removal," Heat Transfer Engineering, Vol. 28, No. 11, pp. 911–923, 2007.
35. Satish G. Kandlikar, "Fundamental issues related to flow boiling in minichannels and microchannels," Experimental Thermal and Fluid Science, Vol. 26 pp. 389–407, 2002.
36. Satish G. Kandlikar, William J. Grande, "Evaluation of Single Phase Flow in Microchannels for High Heat Flux Chip Cooling—Thermohydraulic Performance Enhancement and

Fabrication Technology," Heat Transfer Engineering, Vol. 25, No. 8, pp. 5–16, 2004.

37. Satish G. Kandlikar, William J. Grande, "Evolution of Microchannel Flow Passages--Thermohydraulic Performance and Fabrication Technology," Heat Transfer Engineering, Vol. 24, No. 1, pp. 3–17, 2003.
38. Shankar Krishnan, Suresh V. Garimella, Gregory M. Chrysler, and Ravi V. Mahajan, "Towards a Thermal Moore's Law," IEEE Transactions on Advanced Packaging, vol. 30, NO. 3, pp.462-474, 2007.
39. Sidy Ndao, Yoav Peles, Michael K. Jensen, "Multi-objective thermal design optimization and comparative analysis of electronics cooling technologies," International Journal of Heat and Mass Transfer, Vol. 52, pp. 4317–4326, 2009.
40. Sivakumar D., and Tropea C., "Splashing Impact of a Spray onto a Liquid Film," Physics of Fluids, Vol. 14, No. 12, pp. L85-L88, 2002.
41. T. Kékesi, G. Amberg, L. Prahl Wittberg, "Drop deformation and breakup," International Journal of Multiphase Flow, Vol. 66, pp. 1–10, 2014.
42. Y. A. Cengel, Heat Transfer: A Practical Approach, 2nd ed., McGraw-Hill, 2003
43. Ying-Ming Wanga, Ying Luob, "Integration of correlations with standard deviations for determining attribute weights in multiple attribute decision making," Mathematical and Computer Modeling, Vol. 51, pp.1-12, 2010.

Annexure

##Main function

```
clear all

clc

alt=4;

atr=4;

x=[181 110 9.09 .282;

428 258 12.5 1.1;

58.33 57.2 2.03 .159;

141 10.8 2.17 1.002]


xsqradd(1,atr)=0;

for i=1:alt

    for j=1:atr

        xsqradd(1,j)=(x(i,j))^2+xsqradd(1,j);

    end

end

xsqradd=xsqradd.^.5;

for i=1:alt

    for j=1:atr

        z(i,j)=x(i,j)/xsqradd(1,j);

    end

end

ran=rand(10,atr);

for i=1:10

    add=sum(ran(i,:));

    ranmat(i,:)=ran(i,:)./add;

end
```

```
for i=1:10
    x0 = ranmat(i,:);
    [xf ff flf of]=fminunc(@matfunc, x0);
    weightvalue(i,:)=xf;
    minimumfuncval(i)=ff;
end
[minNum, minIndex] = min(minimumfuncval(:));
[row, col] = ind2sub(size(10), minIndex);
weights=weightvalue(col,:);
 for j=1:atr
            for i=1:alt
                d(i,j)=z(i,j)*weights(1,j);
            end
 end
 bminus(1,atr)=0;
 bplus(1,atr)=0;
 for i=1:alt
    for j=1:atr
            bminus(1,j)=min(d(:,j));
            bplus(1,j)=max(d(:,j));
    end
 end
splus(alt,1)=0;
sminus(alt,1)=0;
 for j=1:atr
    for i=1:alt
            splus(i,1)=(bplus(1,j)-d(i,j))^2+splus(i,1);
            sminus(i,1)=(d(i,j)-bminus(1,j))^2+sminus(i,1);
    end
```

```
 end
 splus=splus.^.5;
 sminus=sminus.^.5;
 for i=1:alt
     r(i,1)=sminus(i,1)/(splus(i,1)+sminus(i,1));
 end
r
```

##Function to be optimized for weights

```
function [lbar] = matfunc(w)
%UNTITLED Summary of this function goes here
%   Detailed explanation goes here
x=[181  110 9.09    .282;
428 258 12.5    1.1;
58.33   57.2    2.03    .159;
141 10.8    2.17    1.002];
alt=4;
atr=4;
for i=1:alt
    for j=1:atr
        if j==2
            a=min(x(:,j));
            b=max(x(:,j));
            z(i,j)=(b-x(i,j))/(b-a);
        elseif j==4
            a=min(x(:,j));
            b=max(x(:,j));
```

```
            z(i,j)=(b-x(i,j))/(b-a);
        else
            a=min(x(:,j));
            b=max(x(:,j));
            z(i,j)=(x(i,j)-a)/(b-a);
        end
     end
end
c=z;
c1=w;
d=zeros(alt,1);
r=zeros(1,atr);
for k=1:atr
    z=c;
    w=c1;
    z(:,k)=[];
    zmod1=z;
    w(:,k)=[];
    wmod=w;
    zmod=c(:,k);
    for j=1:atr-1
            for i=1:alt
                d(i,1)=(zmod1(i,j)*wmod(1,j))+d(i,1);
            end
    end
    zbar=0;
    for i=1:alt
        zbar=zmod(i)+zbar;
    end
```

```
    zbar=zbar / (alt);
    dbar=0;
    for i=1:alt
        dbar=d(i)+dbar;
    end
    dbar=dbar/(alt);
    numadd=0;
    zminussqradd=0;
    dminussqradd=0;
    for i=1:alt
        zminus=zmod(i)-zbar;
        dminus=d(i)-dbar;
        num=zminus * dminus;
        numadd=num+numadd;
        zminussqr=zminus^2;
        zminussqradd=zminussqr+zminussqradd;
        dminussqr =dminus^2;
        dminussqradd=dminussqr+dminussqradd;
    end
    rhozminussqradd=zminussqradd/alt;
    rhosqrtzminussqradd=sqrt(rhozminussqradd);
    rho(k)=rhosqrtzminussqradd;
    den=zminussqradd * dminussqradd;
    densqrt=sqrt(den);
    o=numadd/densqrt;
    r(k)=o;
    sqrtr(k)=sqrt(1-o);
end
z=c;
```

```
w=c1;

t=rho.*sqrtr;

tbar=0;

for j=1:atr

    tbar=t(1,j)+tbar;

end

s=t./tbar;

q=w-s;

l=q.^2;

lbar=0;

for j=1:atr

    lbar=l(1,j)+lbar;

end

end
```

Validation table

Time (ms)	Murat Dinc et al. (2014)	Present research
1.5	0.012986	0.012554
2.5	0.883432	0.874291
3.5	2.046493	1.891475
4.5	3.275783	2.81498
6	4.412266	4.211711

Wall film mass efficiency with angle

time	0 degree	15 degree	45 degree	75 degree
2	8.432628746	8.412045917	7.585437288	13.71888503
4	19.59867778	19.62033846	19.96016852	32.25592065
6	23.38866216	23.45813339	24.25912507	43.26608439

Wall film mass with angle

time	0 degree	15 degree	45 degree	75 degree
2	0.5060547	0.5048184	0.455154	0.8231781

4	2.353225	2.355506	2.396334	3.871104
6	4.211711	4.221209	4.365677	7.788661

Wall film mass at 6ms

6ms			
Height(mm)	2 Nozzles	3 Nozzles	4 Nozzles
10	4.2997190E-06	4.4123030E-06	4.5537440E-06
26	4.2804940E-06	4.3556370E-06	4.4720760E-06
42	4.2668230E-06	4.3282030E-06	4.4257700E-06

Film thickness with nozzles and distance at 6ms

Film thickness			
Distance (mm)	2 Nozzles	3 Nozzles	4 Nozzles
10	1.4970400E-06	1.7010145E-06	1.6686042E-06
26	1.2699219E-06	1.2798968E-06	1.3832126E-06
42	1.0799733E-06	1.2112820E-06	1.0892155E-06

Sauter mean diameter with 2 nozzles

2 nozzles			
time	10mm	26mm	42mm
2	5.6731230E-05	5.6093690E-05	5.6166750E-05
4	3.3602140E-05	3.2854440E-05	3.3423480E-05
6	2.9658430E-05	2.9009070E-05	2.8819800E-05

Sauter mean diameter with 3 nozzles

3 nozzles			
time	10mm	26mm	42mm
2	5.5330070E-05	5.5112560E-05	5.5197900E-05
4	3.4190760E-05	3.3016130E-05	3.2520500E-05
6	3.0595350E-05	2.9511640E-05	2.8788750E-05

Sauter mean diameter with 4 nozzles

4 nozzles			
time	10mm	26mm	42mm
2	5.5251150E-05	5.4604810E-05	5.4948930E-05

4	3.5826560E-05	3.3734590E-05	3.3377040E-05
6	3.2573980E-05	3.0691630E-05	2.9775280E-05

Sauter mean diameter at 2 ms

2 ms			
Distance	2 nozzles	3 nozzles	4 nozzles
10mm	5.6731230E-05	5.5330070E-05	5.5251150E-05
26mm	5.6093690E-05	5.5112560E-05	5.4604810E-05
42mm	5.6166750E-05	5.5197900E-05	5.4948930E-05

Sauter mean diameter at 4 ms

4 ms			
Distance	2 nozzles	3 nozzles	4 nozzles
10mm	3.3602140E-05	3.4190760E-05	3.5826560E-05
26mm	3.2854440E-05	3.3016130E-05	3.3734590E-05
42mm	3.3423480E-05	3.2520500E-05	3.3377040E-05

Sauter mean diameter at 6 ms

6 ms			
Distance	2 nozzles	3 nozzles	4 nozzles
10mm	2.9658430E-05	3.0595350E-05	3.2573980E-05
26mm	2.9009070E-05	2.9511640E-05	3.0691630E-05
42mm	2.8819800E-05	2.8788750E-05	2.9775280E-05